Cells should have inherent folding machinery for denatured proteins. Thus, using reversible cationization, we developed an "in-cell folding" method for a denatured protein, a method to deliver an unfolded protein into cells and let it fold within cells. Using this method, the human tumor-suppressor p53 expressed in *E. coli* as inclusion bodies was successfully delivered into and folded to the active form within p53-null Saos-2 cells.

MATERIALS AND METHODS

Materials. PEI with an average molecular mass of 600 (PEI600) was purchased from Wako Chemical (Osaka, Japan). *N*-Succinimidyl 3-(2-pyridyldithio)propionate (SPDP) was purchased from Pierce (Rockford, IL). An antibody that recognizes the native conformation of wild-type human p53 (anti-native p53 antibody Ab-5) was purchased from Calbiochem (La Jolla, CA). For Western blot analysis, mouse anti-human p53 antibody (anti-p53 antibody Bp53-12, a product of Santa Cruz Biotechnology, Inc.), mouse anti-human tubulin antibody (anti-tubulin antibody), and mouse anti-human β-actin antibody (anti-β-actin antibody) were purchased from Sigma (St. Louis, MO). Mouse anti-p21/wild-type p53-activated fragment 1 antibody clone 6B6 (anti-p21/waf1 antibody 6B6) was purchased from Becton Dickinson (San Jose, CA). For immunofluorescence staining of cells, mouse anti-p21/wild-type p53-activated fragment 1 antibody clone 187 (anti-p21/waf1 antibody 187) was purchased from Santa Cruz Biotechnology, Inc. (Santa Cruz, CA).

Human osteogenic sarcoma-derived Saos-2 cells were obtained from American Type Culture Collection ATCC (Rockville, MD). Normal human fibroblast OUMS-24 cells were those as described elsewhere (*12*). A plasmid encoding human wild-type full-length p53 (pCB6 + p53Pro) was provided by Dr. Karen Vousden.

Synthesis of 3-Aminopropyl Methanethiosulfonate Hydrobromide (APS-Sulfonate) and Pyridyldithiopropionylpolyethylenimine (PEI600-SPDP). APS-sulfonate was synthesized according to the method for the synthesis of 3-(trimethylammonio)propyl methanethiosulfonate bromide [CH_3SO_2-$SCH_2CH_2CH_2N^+(CH_3)_3 \cdot Br^-$] (TAPS-sulfonate) (*7*), except for the use of 3-bromopropylamine hydrobromide instead of (3-bromopropyl)trimethylammonium bromide. APS-sulfonate was obtained as white crystals from ethanol ether in about 80% yield and melted at 121−124 °C. PEI600-SPDP solution was prepared by just mixing a PEI600 solution (200 mg/mL, 0.33 M, pH 8 adjusted by HCl) with SPDP dissolved in ethanol (0.02 M, at a molar ratio of 5:1 PEI600/SPDP). The solution was incubated at room temperature for 20 min and then stored at 4 °C until use.

Protein Expression and Isolation of Inclusion Bodies. The expression plasmid for p53, pBO429, was constructed by the following digestion and ligation steps. The coding region for human wild-type full-length p53 was excised from pCB6 + p53Pro, at the *Nco*I (by partial digestion) and *Bam*HI sites, and the fragment obtained was inserted between the *Nco*I and *Bam*HI sites of an overexpression vector, pET14b (Novagen, WI). Recombinant p53 was expressed in *E. coli* BL21(DE3) (Novagen) harboring pBO429. For overexpression of p53, the cells were cultured at 37 °C in terrific broth containing 200 μg/mL of ampicillin until A_{600} reached 0.8 and were then treated with 0.5 mM isopropyl 1-thio-β-D-galactopyranoside and cultured for another 3 h. The cells were then pelleted and lysed by repeating a freeze/thaw/sonication cycle twice. The isolation of inclusion bodies was performed according to the published procedure (*13*, *14*).

Reversible Cationization of Protein. The recombinant p53 in the inclusion bodies was dissolved in 0.1 M tris(hydroxymethyl)aminomethane (Tris)-HCl buffer at pH 8.6 containing 6 M guanidine-HCl and reduced with 3 mM dithiothreitol (DTT) at 37 °C for 1 h under N_2 atmosphere. Sulfhydryl (SH) groups of p53 were then modified with APS-sulfonate or PEI600-SPDP to give AP-SS-p53 or PEI600-SS-p53, respectively, which were denatured and reversibly cationized p53 proteins containing cationic groups through disulfide (SS) bonds (Figure 1A). Namely, the reaction was initiated by adding 9 mM APS-sulfonate or PEI600-SPDP to the above denatured and reduced p53 solution, and the solution was incubated at 37 °C for 1 h. In the reaction with a relatively large size of PEI600-SPDP, the modification of cysteine residues in p53 was incomplete, probably because of steric hindrance (see below), and the remaining SH groups catalyzed protein polymerization by SH−SS interchange during the following purification procedures. Thus, after cationization with PEI600-SPDP, possible remaining free SH groups were completely protected by the reaction with a smaller size of APS-sulfonate at 3 mM for another 20 min. After cationization, the mixture was dispersed into 10% acetic acid at pH 3 with vigorous stirring. After removal of insoluble materials by centrifugation, reversibly cationized p53 proteins were concentrated by lyophilization, dissolved in a small amount of Milli-Q water, extensively dialyzed against 0.5% acetic acid at pH 4 to remove excess reagents, and purified by a reversed-phase HPLC column (YMC-Pack ODS-A, YMC, Kyoto, Japan) under a linear-gradient elution of acetonitrile from 30 to 40% in the presence of 0.1% HCl. After exchange of the solvent to phosphate-buffered saline (PBS, pH 7.4) by dialysis or a PD-10 column (Amersham Bioscience, Buckinghamshire, U.K.), the purified reversibly cationized p53 proteins, AP-SS-p53 and PEI600-SS-p53, were used for biological experiments. The number of cysteine residues modified with PEI600 in PEI600-SS-p53 was determined by MALDI−TOF mass spectrometry with a Perspective Voyager-DE PRO mass spectrometer.

As a control protein, bovine serum albumin (BSA) was also reversibly cationized with PEI600-SPDP to give PEI600-SS-BSA, which is a reduced and denatured BSA derivative reversibly cationized with PEI through SS bonds. That is, BSA was reduced with DTT in 0.525 M Tris-HCl (pH 8.6) containing 8 M urea (*6*) and reversibly cationized with PEI600-SPDP for 30 min. In this case, possible remaining SH groups were irreversibly modified by incubation with iodoacetamide for 15 min, and the exchange of the solvent to PBS was carried out by a PD10 column.

Folding Ability of Reversibly Cationized p53 Protein In Vitro. To test the spontaneous folding ability of denatured and reversibly cationized p53 proteins under cytosolic redox conditions, rapid dilution of PEI600-SS-p53 into PBS (pH 7.4) containing 2.5 mM reduced glutathione and 0.05 mM oxidized glutathione at a final protein concentration of 20 μg/mL at 20 °C was carried out. Aliquots were withdrawn at appropriate intervals and subjected to sodium dodecyl sulfate−polyacrylamide gel electrophoresis (SDS−PAGE)

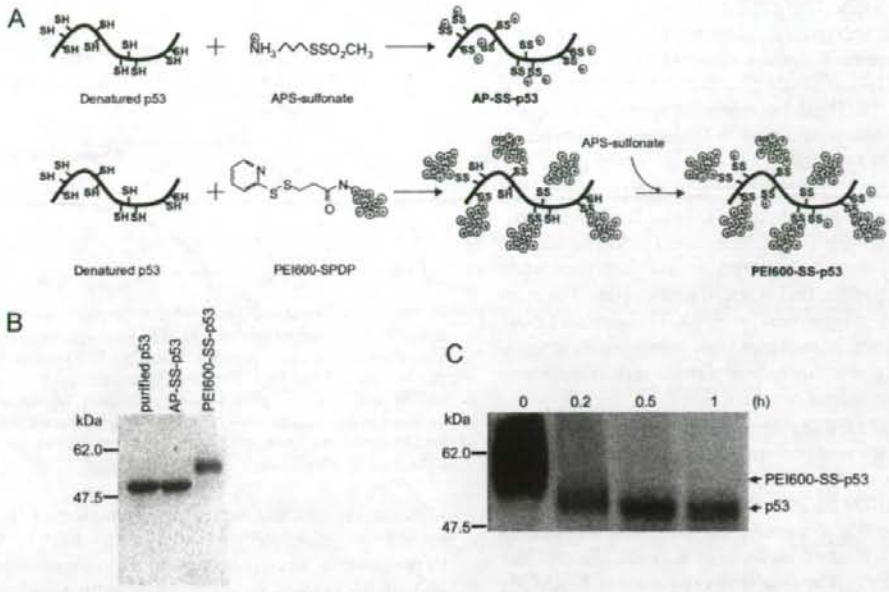

FIGURE 1: Preparation and characterization of denatured and reversibly cationized p53 proteins. (A) Reduced and denatured p53 obtained from inclusion bodies was reversibly cationized in mixed disulfide bonds with APS-sulfonate to give AP-SS-p53 or with PEI600-SPDP followed by APS-sulfonate to give PEI600-SS-p53. (B) SDS−PAGE analysis of purified recombinant p53 and its derivatives (AP-SS-p53 and PEI600-SS-p53) on 10% polyacrylamide gel under nonreducing conditions. The gel was stained with Coomassie Briliant Blue R250. (C) Time-dependent reduction of PEI600-SS-p53 in vitro under cytosolic redox conditions. PEI600-SS-p53 was incubated in a mixture of 2.5 mM reduced glutathione and 0.05 mM oxidized glutathione at pH 7.4 and 20 °C for indicated periods and subjected to SDS−PAGE followed by Western blot analysis using mouse anti-p53 antibody Bp53-12 as a primary antibody and horseradish peroxidase-conjugated goat anti-mouse IgG antibody as a secondary antibody. Details are given in the text.

under nonreducing conditions. The gel was blotted onto a nitrocelulose membrane for Western blot analysis using mouse anti-p53 antibody Bp53-12 as a primary antibody, horseradish peroxidase-conjugated goat anti-mouse IgG antibody (Cell Signaling) as a secondary antibody, and an enhanced chemiluminescence kit (Amersham Biosciences).

Cell Culture and Protein Transduction. p53-null human osteosarcoma Saos-2 and Saos-2/simian virus 40 large-T antigen (SVLT) cells and normal human fibroblast OUMS-24 cells (*12*) were cultured in Dulbecco's modified Eagle's medium (DMEM, Nissui Pharmaceutical, Tokyo, Japan) containing 10% fetal bovine serum (FBS, Sigma). For establishment of Saos-2/SVLT cells, a plasmid encoding SVLT and a G418 resistance marker was introduced into Saos-2 cells using LipofectAMIN 2000 (Invitrogen, CA), and a stably transfected clone was isolated. All cells were cultured in a humidified 5% CO_2 incubator at 37 °C. For protein transduction experiments, about 80% confluent cells were washed once with serum-free medium and then a cationized protein was added under serum-free conditions. After incubation for 1 h at 37 °C, FBS was added at a final concentration of 10% and cells were further incubated for appropriate periods.

Immunoprecipitation and Western Blot Analysis. Cell lysates were prepared using lysis buffer containing 40 mM Tris-HCl at pH 7.4, 1% TritonX-100, 150 mM NaCl, 1 mM ethylenediaminetetraacetic acid (EDTA), 1 mM ethyleneglycol bis(2-aminoethylether)tetraacetic acid (EGTA), 1 mM DTT, and 10% glycerol and were clarified by centrifugation. For immunoprecipitation, cell lysates were precleared with protein G-Sepharose beads (Amersham Biosciences) and then incubated with anti-native p53 antibody Ab-5 for 1 h at 4 °C on a rotating rocker, followed by an additional incubation with protein G-Sepharose beads for 1 h. The immune complexes as well as cell extracts were subjected to SDS−PAGE and transferred onto nitrocellulose membranes. For Western blot analysis, after blocking with 10% skim milk powder and 6% glycine dissolved in PBS, membranes were incubated with anti-p53 antibody Bp53-12, anti-p21/waf1 antibody 6B6, anti-β-actin antibody, or anti-tubulin antibody as primary antibodies. Each specific antibody binding was detected with horseradish peroxidase-conjugated goat anti-mouse IgG antibody and an enhanced chemiluminescence kit as described above.

Cross-Linking Analysis. For analysis of the quaternary structure of exogenously added p53, cells were treated with 1 mM glutaraldehyde for 10 min at 25 °C to preserve the molecular interaction by cross-linking. The reaction was terminated by the addition of 0.1 M glycine. Cell lysates prepared were analyzed by Western blot analysis using anti-p53 antibody Bp53-12. The normal human fibroblast OUMS-24 cells were incubated under confluent or serum-starved conditions for 24 h or the cells were treated with 10 μM 4-nitroquinoline 1-oxide (4NQO) for 6 h. These cells were used as positive controls. Saos-2 and OUMS-24 cells incubated without additives or Saos-2 cells incubated with PEI600-SS-BSA were used as negative controls.

Immunofluorescence Staining. Cells were fixed with 4% paraformaldehyde for 1 h at room temperature and then permeabilized with 70% ethanol at −20 °C. Immunofluorescence staining for exogenously added p53 or endogenously expressed p21/waf1 was performed by treatment of cells with

mouse anti-p53 antibody Bp53-12 or mouse anti-p21/waf1 antibody 187, respectively, followed by treatment with tetramethylrhodamine B isothiocyanate (TRITC)-conjugated goat anti-mouse IgG antibody (Sigma). Nuclei were stained with Hoechst 33258 (Dojin Laboratories, Kumamoto, Japan). The cells were observed under a fluorescent microscope (IX71-22FL/PH, Olympus).

Northern Blotting. Total RNA was isolated using the guanidium thiocyanate method (*15*). Total RNA was separated by electrophoresis (15 μg/lane) in a 1% formaldehyde-agarose gel and then transferred to a nylon membrane (Nytran-Plus, Schleicher and Schuell, Keene, NH). The blots were probed with gel-purified [γ-^{32}P]dCTP-labeled cDNAs for p21/waf1 mRNA. Membranes were subsequently stripped and reprobed for glyceraldehyde-3-phosphate dehydrogenase (GAPDH) for normalization.

Electrophoresis Mobility Shift Assay. An electrophoresis mobility shift assay was performed as described by Nakano et al. (*16*) using crude nuclear extracts from cells treated with 100 nM PEI600-SS-p53, 100 nM PEI600-SS-BSA, or 10 μM 4NQO for 6 h. We used a double-strand oligonucleotide for the p53-binding element as a probe (Santa Cruz Biotechnology, Inc.). The consensus sequence is 5′-TACAGAACATGTCTAAGCATGCTGGGG-3′. The [γ-^{32}P]dATP-labeled probe was mixed with crude nuclear extracts of Saos-2 or OUMS-24 cells, incubated for 1 h at 4 °C, and electrophoresed in a 5% polyacrylamide gel under nondenaturing conditions.

Apoptosis Analysis with DNA-Ladder Formation. The cells at various stages were harvested and incubated with lysis buffer containing 10 mM Tris-HCl at pH 7.4, 5 mM EDTA, and 1% TritonX-100 for 20 min on ice. The supernatant containing DNA fragments was incubated with 10 μg/mL RNase A for 1 h at 37 °C. After further incubation with 20 μg/mL proteinase K for 1 h at 37 °C, samples were washed with phenol−chloroform and DNA was precipitated with ethanol. Recovered DNA was electrophoresed on 2% agarose gel and stained with ethidium bromide.

RESULTS

Preparation of Denatured and Reversibly Cationized p53. As summarized in Figure 1A, reversibly cationized p53 proteins were prepared from inclusion bodies dissolved in 6 M guanidine-HCl by alkylsulfidation of sulfhydryl groups with APS-sulfonate and PEI600-SPDP, respectively. Because the modification of p53 with PEI600-SPDP was found to be incomplete (approximately 6 of 10 cysteine residues) probably because of steric hindrance, the remaining 4 free sulfhydryl groups were completely protected with a smaller size of APS-sulfonate. Formation of mixed disulfides with positively charged side-chain groups, especially with PEI, in the polypeptide chain resulted in slower migration on SDS−PAGE under nonreducing conditions (Figure 1B). Both cationized p53 proteins (AP-SS-p53 and PEI600-SS-p53) showed good solubility in water, especially at acidic pH values, because of an increase in the net positive charge by protonation of carboxyl groups. We have confirmed that reversibly cationized p53 proteins remained soluble in 0.5% acetic acid for more than 6 months at 4 °C.

Upon rapid dilution in vitro, reduced p53 purified from inclusion bodies has been reported to have the ability to fold into the biologically active conformation (*17*). Thus, for reversibly cationized p53 proteins to fold in vivo, it is important that they are able to revert to unprotected reduced p53 under cytosol-mimic redox conditions (50:1 reduced glutathione/oxidized glutathione) (*18*). As mentioned above (Figure 1B), PEI600-SS-p53 migrates slower than p53 on SDS−PAGE, and hence, reduction of PEI600-SS-p53 can be monitored. Upon dilution of PEI600-SS-p53 into the redox buffer, PBS (pH 7.4) containing 2.5 mM reduced glutathione and 0.05 mM oxidized glutathione, at a final protein concentration of 20 μg/mL at 20 °C, rapid removal of protecting groups by reduction was observed, and this reduction seemed to be completed in about 1 h to give unprotected p53 (Figure 1C). No precipitation was observed during the process. These results suggest that the reversibly cationized p53 proteins can be reduced to free p53 if they internalized into the cytosol and therefore might fold into the native p53.

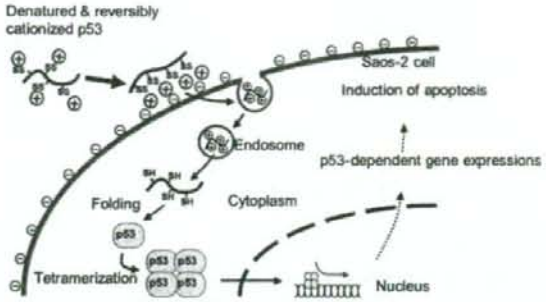

FIGURE 2: Schematic diagram of the "in-cell folding" method for the p53 tumor-suppressor protein. The essential steps for externally added denatured and reversibly cationized p53 to express the native protein functions in Saos-2 cells (electrostatic cell-surface adsorption and/or endosome accumulation, reduction of disulfide bonds because of the release to cytosol, folding and tetramer formation, localization into the nucleus, induction of p53 target genes, and induction of apoptosis of cells) are depicted.

Intracellular Protein Delivery of Reversibly Cationized p53. To investigate whether reversibly cationized p53 proteins could internalize into cells and simultaneously fold into the biologically active structure, we tested essential steps of known p53-dependent cellular responses, as depicted in Figure 2. We employed Saos-2 cells for this assay, because of the lack of endogenous p53 (*19*).

As visualized by immunofluorescence staining, Saos-2 cells showed marked cellular uptake of p53 when exposed to either AP-SS-p53 or PEI600-SS-p53 for 6 h (Figure 3A). Although these fluorescence patterns observed using a fluorescence microscope did not enable p53 internalized in cytoplasmic compartments to be distinguished from the cell-surface associated one, observation of PEI600-SS-p53-treated cells using a confocal laser-scanning microscope indicated that fluorescence was mostly present inside cells (data not shown). The more cationic PEI600-SS-p53 seemed more effective in cellular uptake than did AP-SS-p53 (Figure 3A).

We have previously demonstrated that PEI-cationized proteins enter living cells and have shown that the major mechanism of the protein internalization is endocytotic uptake and subsequent release into the cytosol from endosomes (*4*, *5*). If the reversibly cationized p53 proteins internalize via an endocytotic pathway, the entrapped proteins

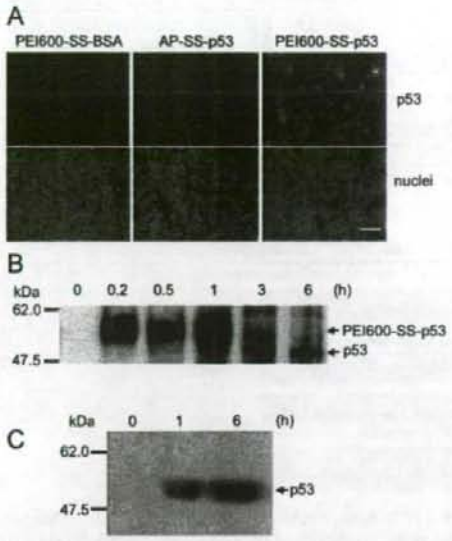

FIGURE 3: Cellular uptake, reduction, and folding of exogenously added reversibly cationized p53 proteins to Saos-2 cells. (A) Saos-2 cells were incubated with 100 nM PEI600-SS-BSA, AP-SS-p53, or PEI600-SS-p53 for 6 h, fixed, immunostained with mouse anti-p53 antibody Bp53-12 and TRITC-conjugated anti-mouse IgG antibody, and observed under a fluorescent microscope (upper panels). Nuclei stained with Hoechst 33258 are also indicated (lower panels). The scale bar is equivalent to 50 μm. (B) Time course of the reduction of PEI600-SS-p53 in cells. Saos-2 cells were incubated with 100 nM PEI600-SS-p53 for indicated periods, and the reduction of PEI600-SS-p53 was analyzed by Western blot analysis with anti-p53 antibody Bp53-12 after SDS−PAGE of cell lysates under nonreducing conditions. (C) Detection of intracellularly folded p53. After incubation of Saos-2 cells with 100 nM PEI600-SS-p53 for indicated periods, folded p53 was collected from cell lysates by immunoprecipitation using anti-native p53 antibody Ab-5 and protein G-Sepharose beads. The precipitates were then electrophoresed by SDS−PAGE under reducing conditions, blotted to nitrocellulose membranes, and analyzed by Western blot analysis with anti-p53 antibody Bp53-12.

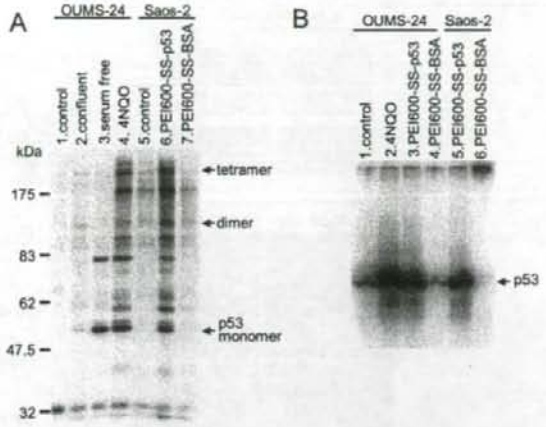

FIGURE 4: Analysis of the quaternary structure and DNA binding of folded p53. (A) Oligomeric states of internalized p53 in cells determined by cross-linking analysis. Normal human fibroblast OUMS-24 cells were incubated under nonconfluent conditions for 6 h (negative control, lane 1), under confluent conditions for 24 h (positive control, lane 2), or under serum-starved conditions for 24 h (positive control, lane 3) or were treated with 10 μM 4NQO for 6 h (positive control, lane 4). p53-null Saos-2 cells were incubated without additives (negative control, lane 5), with 100 nM PEI600-SS-p53 (lane 6), or with PEI600-SS-BSA (negative control, lane 7) for 6 h. The cells were treated with 1 mM glutaraldehyde and then lysed, and cell lysates were analyzed by Western blot analysis using anti-p53 antibody Bp53-12. Arrows indicate positions of the tetramer, dimer, and monomer of p53, which were separately determined by using p53 cross-linked with glutaraldehyde in vitro (data not shown). (B) Electrophoresis mobility shift assay of the p53-binding element with internalized p53 in cells. Crude nuclear extracts from OUMS-24 cells incubated without additives (lane 1), with 10 μM 4NQO (lane 2), with 100 nM PEI600-SS-p53 (lane 3), or with 100 nM PEI600-SS-BSA (lane 4) for 6 h or those from Saos-2 cells incubated with 100 nM PEI600-SS-p53 (lane 5) or 100 nM PEI600-SS-BSA (lane 6) for 6 h were incubated with [γ-^{32}P]dATP-labeled double-strand oligonucleotide for the p53-binding element for 1 h at 4 °C and then electrophoresed in a 5% polyacrylamide gel under nondenaturing conditions. The [γ-^{32}P]dATP-labeled p53-binding element in the gel was detected autoradiographically. Arrow indicates the position of p53.

in the endosome would remain inactive because disulfide bonds are scarcely reduced under endosomal oxidative conditions, but they might fold to the active conformation in the cytosol because disulfide bonds are readily reduced under cytosolic reductive conditions (Figure 1C). Thus, reduction of mixed disulfide bonds in reversibly cationized p53 proteins should be good proof of their cytosolic release. Western blot analysis of SDS−PAGE for PEI600-SS-p53-treated Saos-2 cells indicated that the band corresponding to PEI600-SS-p53 because of cell-surface adsorption and/or endosome accumulation was the main band for the first 1 h of incubation but that the band corresponding to reduced p53 because of cytosolic release became the main band after 3 and 6 h of incubation (Figure 3B).

To confirm time-dependent folding of reversibly cationized p53 proteins in Saos-2 cells, folded p53 in the cell lysate was immunoprecipitated with a specific antibody recognizing the native conformation (anti-native p53 antibody Ab-5) after incubation of cells with 100 nM PEI600-SS-p53 for 1 and 6 h, and the precipitates were analyzed by Western blotting analysis using anti-p53 antibody Bp53-12 (Figure 3C). Time-dependent formation of p53 assuming native conformation was clearly observed, being well-correlated with the reduction of PEI600-SS-p53 in the cytosol (Figure 3B). All of these observations suggest that exogenously added reversibly cationized p53 proteins are rapidly adsorbed on the cell surface by the electrostatic interaction, endocytozed by cells up to 1 h at 37 °C, and more slowly released into the cytosol, where reduction of mixed disulfide bonds followed by folding to the biologically active form takes place.

Quaternary Structure and Specific DNA Binding of Intracellularly Folded p53. The transcriptional activity of p53 has been reported to be associated with a tetrameric form that binds DNA in a sequence-specific fashion to activate the transcription of target genes (*20*−*23*). To confirm the formation of tetrameric p53 when delivered into cells as described above, we performed cross-linking experiments with glutaraldehyde as a cross-linking agent to fix the protein quaternary structure. As shown in Figure 4A, the electrophoretic pattern obtained from PEI600-SS-p53-treated Saos-2 cells indicated the presence of a covalently cross-linked p53 dimer and tetramer including possibly their degraded products (lane 6). No such pattern was obtained from Saos-2 cells treated without cationized protein (one negative control, lane

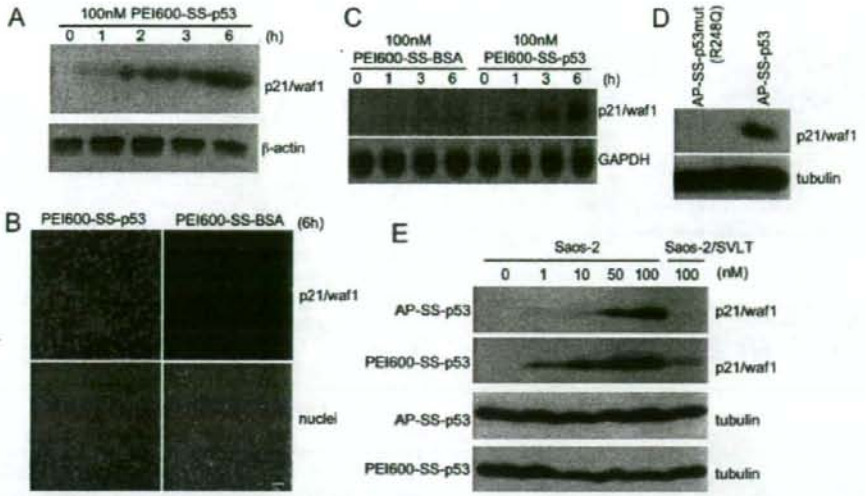

FIGURE 5: Induction of the p53-dependent gene expression of p21/waf1. Saos-2 cells were incubated with 100 nM PEI600-SS-p53 or PEI600-SS-BSA for indicated periods, and induction of p21/waf1 was examined at the protein level (A and B) or mRNA level (C). (A) Western blot analysis of the time-dependent expression of the p21/waf1 protein in Saos-2 cells by treatment with 100 nM PEI600-SS-p53. Expression of p21/waf1 (upper panel) was examined by SDS−PAGE of cell lysates and Western blot analysis with anti-p21/waf1 antibody 6B6. The expression level of β-actin (lower panel) was examined by reprobing using anti-β-actin antibody for normalization. (B) Saos-2 cells were incubated with 100 nM PEI600-SS-p53 (left panels) or PEI600-SS-BSA (right panels) for 6 h, fixed, immunostained with mouse anti-p21/waf1 antibody 187 and TRITC-conjugated anti-mouse IgG antibody, and then observed under a fluorescent microscope (upper panels). Nuclei stained with Hoechst 33258 are also indicated (lower panels). The bar indicates 80 μm. (C) Northern blot analysis for examination of the time-dependent expression of p21/waf1 mRNA in PEI600-SS-p53-treated Saos-2 cells. Total RNAs isolated from cells treated with 100 nM PEI600-SS-BSA or PEI600-SS-p53 for indicated periods were separated by electrophoresis and transferred to nylon membranes. The blots were probed with [γ-^{32}P]dCTP-labeled cDNAs for p21/waf1 (upper panel). Membranes were subsequently stripped and reprobed for GAPDH for normalization (lower panel). (D) Transactivation activity of the p53-dependent p21/waf1 protein expression. Saos-2 cells were incubated with 100 nM AP-SS-p53 (upper panel, right) or transactivation-deficient AP-SS-p53 mutant [AP-SS-p53mut (R248Q)] (upper panel, left) for 6 h and analyzed by Western blot analysis using anti-p21/waf1 antibody 6B6. Tubulin was employed for normalization (lower panel). (E) Dose dependence of p21/waf1 protein expression in reversibly cationized p53-treated Saos-2 cells and lack of p53 function in reversibly cationized p53-treated Saos-2/SVLT cells. Saos-2 cells and Saos-2/SVLT cells that express SVLT suppressing the p53 function were incubated with AP-SS-p53 or PEI600-SS-p53 at indicated concentrations for 6 h. After SDS−PAGE of cell lysates, expression levels of p21/waf1 were analyzed by Western blot analysis using anti-p21/waf1 antibody 6B6 (top panel for AP-SS-p53 and second-to-top panel for PEI600-SS-p53). Tubulin was employed for normalization (bottom and second-to-bottom panels).

5) or from Saos-2 cells treated with cationized BSA (another negative control, lane 7). However, the same pattern was obtained from normal OUMS-24 cells that the endogenous p53 level was upregulated by 4NQO (a positive control, lane 4) (*12*, *24*). These results suggest that externally added reversibly cationized p53 folds intracellularly to a tetrameric form. Interestingly, the pattern obtained from confluent OUMS-24 cells (one of the positive controls, lane 2) seemed similar to the pattern from PEI600-SS-p53-treated cells, although the level of tetrameric p53 was very low, while the pattern obtained from serum-starved OUMS-24 cells (another positive control, lane 3) seemed different from those of other positive controls in the distribution of p53 oligomers and degraded products. The growth-arrested state in serum-starved cells might not be the same as that in confluent cells.

Next, we investigated the specific binding ability of intracellularly folded p53 to a DNA fragment of the p53-binding element. As shown in Figure 4B, the nuclear extract obtained from Saos-2 cells treated with PEI600-SS-p53 for 6 h contained p53 showing specific binding activity against the labeled DNA fragment (lane 5). Similar results were also obtained by using nuclear extracts from 4NQO-treated OUMS-24 cells (positive control, lane 2) and from PEI600-SS-p53-treated OUMS-24 cells (lane 3). The nuclear extract from OUMS-24 cells incubated without cationized protein (lane 1) or with cationized BSA (lane 4) showed a background level of active p53 in the cells. The nuclear extract from cationized BSA-treated Saos-2 cells did not give the band corresponding to p53 (lane 6). These results imply that the intracellularly folded p53 was translocated to the nucleolus as a biologically active tetramer when cells were incubated with PEI600-SS-p53 for 6 h.

Induction of Intracellularly Delivered p53-Dependent Gene Expression. If exogenously added reversibly cationized p53 proteins express their transcriptional activity, one of the known p53 target gene products, p21/waf1, should be upregulated in Saos-2 cells (*20*, *25*). Thus, we examined the effect of treatment of Saos-2 cells with AP-SS-p53 or PEI600-SS-p53 on the expression of p21/waf1 and found that was the case (Figure 5). Time-dependent expression of p21/waf1 was examined by adding 100 nM PEI600-SS-p53 to the culture medium of Saos-2 cells. The cells were harvested several times for Western blot analysis up to 6 h after the addition of PEI600-SS-p53. The protein level of p21/waf1 was gradually elevated by this treatment (Figure 5A). Immunofluorescence experiments revealed that the expression of p21/waf1 was induced in approximately 60% of cells by this treatment for 6 h but not by treatment with PEI600-SS-BSA (Figure 5B). The same was true when the induction of p21/waf1 was monitored by the mRNA level (Figure 5C). Another reversibly cationized p53 protein, AP-SS-p53, also induced p21/waf1 expression in Saos-2 cells,

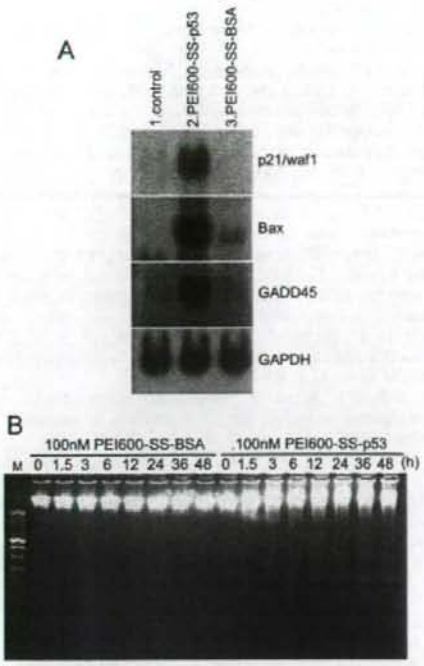

FIGURE 6: Biological effects of introduced p53 on Saos-2 cells. (A) Saos-2 cells were treated without additives (control, lane 1), with 100 nM PEI600-SS-p53 (lane 2), or with PEI600-SS-BSA (lane 3) for 6 h, and transcriptional activation of p53-dependent apoptotic genes (p21/waf1, Bax, and GADD45) was examined by Northern blot analysis. GAPDH was employed for normalization. (B) DNA fragmentation in Saos-2 cells treated with PEI600-SS-p53. After incubation of Saos-2 cells with 100 nM PEI600-SS-p53 or PEI600-SS-BSA for indicated periods, the respective DNAs were extracted and analyzed by electrophoresis on a 2% agarose gel. The gel was stained with ethidium bromide. M indicates molecular markers (the left most lane).

but p21/waf1 expression was not induced when cells were treated with reversibly cationized transactivation-deficient AP-SS-p53 mutant (R248Q) (*26*) (Figure 5D). The latter result is consistent with the failure of AP-SS-p53 or PEI600-SS-p53 to induce p21/waf1 in Saos-2/SVLT cells that express SVLT suppressing p53 function by specific binding (*27*) (Figure 5E). We further compared AP-SS-p53 and PEI600-SS-p53 for dose dependency to the induction of p21/waf1. The more cationic PEI600-SS-p53 showed more efficient activity than did AP-SS-p53 as seen in the treatment with 1 nM for 6 h (Figure 5E). These results demonstrated that exogenous p53 delivered by this method is a highly potent inducer of the target gene expression.

Induction of Apoptosis by Intracellularly Delivered p53-Dependent Gene Expression. Because it has been reported that induction of p53 expression in Saos-2 cells at a low level induces growth arrest but at a high level induces apoptosis (*28*), we analyzed apoptotic gene expression in PEI600-SS-p53-treated Saos-2 cells. Treatment with 100 nM PEI600-SS-p53 but not with 100 nM PEI600-SS-BSA for 6 h caused transcriptional activation of p53-dependent apoptotic genes (p21/waf1, Bax, and GADD45) in Saos-2 cells (Figure 6A). These results were supported by apoptotic DNA-ladder formation in PEI600-SS-p53-treated cells compared with that in PEI600-SS-BSA-treated cells (Figure 6B).

DISCUSSION

The living cell membrane poses a substantial hurdle for exogenous protein to express its function inside cells. To overcome this limitation, a variety of new methodologies to deliver functional proteins into cells are being studied actively. The new methodologies include "protein cationization methods". Methods using 8−35 amino-acid-long peptides called "protein transduction domains" (PTDs) are the most popular (*29*−*35*). PTDs derived from human immunodeficiency virus-transactivator of transcription (HIV-TAT) (*30*, *32*), herpes simplex virus-structural protein VP22 (HSV-VP22) (*31*), and antennapedia (*29*) or synthetic PTDs (*33*−*35*) are characterized by a high content of positively charged arginine and lysine residues, which are potentially important for association with the negatively charged cell-surface membrane by electrostatic interaction followed by internalization into cells by endocytosis (*36*, *37*) or macropinocytosis (*38*). Chemical cationization methods developed by us (*3*−*5*) are also included in this category. A cationic lipid-based carrier system (*39*), virus envelope vector (*40*), and PEI-cationized carrier systems (*5*) have also been proposed. Although these current protein transduction techniques seem promising for laboratory investigations and therapeutic applications, proteins to be delivered into cells require sufficient solubility. Because denatured proteins are hardly soluble in physiological aqueous solutions, detergents or denaturants toxic for living cells are generally used to solubilize them. In the present study, we showed that the denatured form of the reversibly cationized p53 protein was not only soluble in physiological solutions but also active for transduction into living cells to express its functions inside cells because of simultaneous folding. We call this protein transduction method the "in-cell folding" technique. This technique would be of great value especially when proteins to be delivered into cells are not easily available as biologically active conformations in vitro.

Because mutations in p53 are among the most common genetic events in the development of human cancer (*41*), many studies have been carried out to evaluate viral vector-mediated p53 gene delivery for gene therapy (*42*). Approaches for protein transduction therapy using a PTD peptide fused to folded p53 have also been carried out and have been shown to be useful to inhibit the proliferation of cancer cells (*43*−*45*). Although a protein transduction method allows the protein to function in cells transiently, PEI600-SS-p53 could induce p53-target genes only at 1 nM (Figure 5E), suggesting that the method would be effective at limited doses to inhibit cancer cell growth in therapeutic applications.

In this study, we used APS-sulfonate and PEI600-SPDP to cationize denatured p53 (Figure 1A). Both reagents possess moieties with common characteristics, a SH-selective and rapid modifying moiety (methanethiosulfonyl or dithiopyridyl group) and a cationic side-chain moiety (amine or polyamine group). Thus, in the reaction with these reagents, positive charges were introduced into 10 cysteine residues (that is, 10 free SH groups) of p53 through the formation of mixed disulfide bonds to give AP-SS-p53 or PEI600-SS-p53. As shown in Figure 1C, AP-SS-p53 and PEI600-SS-p53 were equivalent to reduced p53 in the SS−SH interchange reaction under cytosolic redox conditions. In other words, denatured

AP-SS-p53, PEI600-SS-p53, and reduced p53 have equivalent folding abilities in the cytosol.

If charged residues at neutral pH are assumed to be only Asp(−1), Glu(−1), Lys(+1), and Arg(+1) for simplicity, the net charge of wild-type p53 is calculated to be −4. APS-sulfonate and PEI600-SPDP can introduce positive charges of +1 and +13.6, respectively, into every cysteine residue. As mentioned above, PEI600-SS-p53 contained approximately six and four cysteine residues modified with PEI600-SPDP and APS-sulfonate, respectively. Thus, net charges of AP-SS-p53 and PEI600-SS-p53 were calculated to be +6 and +81.6, respectively. We previously showed that the net positive charge of proteins correlated well with their efficiency in protein transduction (*2*, *3*, *46*). Consistent with this previous observation, PEI600-SS-p53 seemed to be more effective than AP-SS-p53 (Figures 3A and 5E).

Although various recombinant protein production systems or in vitro translation systems are now available, there is no guarantee that a large amount of biologically active products will be yielded. However, denatured proteins can be easily obtained as inclusion bodies in good yield if an *E. coli* expression system is used. The results presented here demonstrated the possibility of the "in-cell folding" technique; that is, reversibly cationized unfolded proteins could internalize into living cells and simultaneously fold to biologically active conformations. Because many newly synthesized proteins in the cytosol require involvement of complex cellular machinery such as chaperones and processing enzymes as well as input of metabolic energy to reach their native states (*47*) and because such machinery is not easily utilized in vitro, the strategy of "in-cell folding" may be reasonable in some cases. Thus, the "in-cell folding" technique may greatly enhance the utility of a protein expression system, yielding unfolded proteins such as hardly soluble inclusion bodies when protein transduction into living cells is attempted.

REFERENCES

1. Kumagai, A. K., Eisenberg, J. B., and Pardridge, W. M. (1987) Absorptive-mediated endocytosis of cationized albumin and a β-endorphin-cationized albumin chimeric peptide by isolated brain capillaries. Model system of blood-brain barrier transport, *J. Biol. Chem. 262*, 15214−15219.
2. Futami, J., Maeda, T., Kitazoe, M., Nukui, E., Tada, H., Seno, M., Kosaka, M., and Yamada, H. (2001) Preparation of potent cytotoxic ribonucleases by cationization: Enhanced cellular uptake and decreased interaction with ribonuclease inhibitor by chemical modification of carboxyl groups, *Biochemistry 40*, 7518−7524.
3. Futami, J., Nukui, E., Maeda, T., Kosaka, M., Tada, H., Seno, M., and Yamada, H. (2002) Optimum modification for the highest cytotoxicity of cationized ribonuclease, *J. Biochem. 132*, 223−228.
4. Futami, J., Kitazoe, M., Maeda, T., Nukui, E., Sakaguchi, M., Kosaka, J., Miyazaki, M., Kosaka, M., Tada, H., Seno, M., Sasaki, J., Huh, N. H., Namba, M., and Yamada, H. (2005) Intracellular delivery of proteins into mammalian living cells by polyethylenimine-cationization, *J. Bioeng. Biosci. 99*, 95−103.
5. Kitazoe, M., Murata, H., Futami, J., Maeda, T., Sakaguchi, M., Miyazaki, M., Kosaka, M., Tada, H., Seno, M., Huh, N. H., Namba, M., Nishikawa, M., Maeda, Y., and Yamada, H. (2005) Protein transduction assisted by polyethylenimine-cationized carrier proteins, *J. Biochem. 137*, 693−701.
6. Yamada, H., Seno, M., Kobayashi, A., Moriyama, T., Kosaka, M., Ito, Y., and Imoto, T. (1994) An *S*-alkylating reagent with positive charges as an efficient solubilizer of denatured disulfide-containing proteins, *J. Biochem. 116*, 852−857.
7. Inoue, M., Akimaru, J., Nishikawa, T., Seki, N., and Yamada, H. (1998) A new derivatizing agent, trimethylammoniopropyl methanethiosulphonate, is efficient for preparation of recombinant brain-derived neurotrophic factor from inclusion bodies, *Biotechnol. Appl. Biochem. 28*, 207−213.
8. Seno, M., DeSantis, M., Kannan, S., Bianco, C., Tada, H., Kim, N., Kosaka, M., Gullick, W. J., Yamada, H., and Salomon, D. S. (1998) Purification and characterization of a recombinant human cripto-1 protein, *Growth Factors 15*, 215−229.
9. Mallorqui-Fernandez, G., Pous, J., Peracaula, R., Aymami, J., Maeda, T., Tada, H., Yamada, H., Seno, M., de Llorens, R., Gomis-Ruth, F. X., and Coll, M. (2000) Three-dimensional crystal structure of human eosinophil cationic protein (RNase 3) at 1.75 Å resolution, *J. Mol. Biol. 300*, 1297−1307.
10. Miura, K., Doura, H., Aizawa, T., Tada, H., Seno, M., Yamada, H., and Kawano, K. (2002) Solution structure of betacellulin, a new member of EGF-family ligands, *Biochem. Biophys. Res. Commun. 294*, 1040−1046.
11. Newton, D. L., Futami, J., Ruby, D., and Rybak, S. M. (2003) Construction and characterization of RNase-based targeted therapeutics, *Methods Mol. Biol. 207*, 283−304.
12. Bai, L., Mihara, K., Kondo, Y., Honma, M., and Namba, M. (1993) Immortalization of normal human fibroblasts by treatment with 4-nitroquinoline 1-oxide, *Int. J. Cancer 53*, 451−456.
13. Futami, J., Tsushima, Y., Tada, H., Seno, M., and Yamada, H. (2000) Convenient and efficient in vitro folding of disulfide-containing globular protein from crude bacterial inclusion bodies, *J. Biochem. 127*, 435−441.
14. Futami, J., Tada, H., Seno, M., Ishikami, S., and Yamada, H. (2000) Stabilization of human RNase 1 by introduction of a disulfide bond between residues 4 and 118, *J. Biochem. 128*, 245−250.
15. Chirgwin, J. M., Przybyla, A. E., MacDonald, R. J., and Rutter, W. J. (1979) Isolation of biologically active ribonucleic acid from sources enriched in ribonuclease, *Biochemistry 18*, 5294−5299.
16. Nakano, K., Mizuno, T., Sowa, Y., Orita, T., Yoshino, T., Okuyama, Y., Fujita, T., Ohtani-Fujita, N., Matsukawa, Y., Tokino, T., Yamagishi, H., Oka, T., Nomura, H., and Sakai, T. (1997) Butyrate activates the WAF1/Cip1 gene promoter through Sp1 sites in a p53-negative human colon cancer cell line, *J. Biol. Chem. 272*, 22199−22206.
17. Bell, S., Hansen, S., and Buchner, J. (2002) Refolding and structural characterization of the human p53 tumor suppressor protein, *Biophys. Chem. 96*, 243−257.
18. Hwang, C., Sinskey, A. J., and Lodish, H. F. (1992) Oxidized redox state of glutathione in the endoplasmic reticulum, *Science 257*, 1496−1502.
19. Diller, L., Kassel, J., Nelson, C. E., Gryka, M. A., Litwak, G., Gebhardt, M., Bressac, B., Ozturk, M., Baker, S. J., Vogelstein, B., and Friend, S. H. (1990) p53 functions as a cell cycle control protein in osteosarcomas, *Mol. Cell. Biol. 10*, 5772−5781.
20. el-Deiry, W. S., Tokino, T., Velculescu, V. E., Levy, D. B., Parsons, R., Trent, J. M., Lin, D., Mercer, W. E., Kinzler, K. W., and Vogelstein, B. (1993) WAF1, a potential mediator of p53 tumor suppression, *Cell 75*, 817−825.
21. Halazonetis, T. D., and Kandil, A. N. (1993) Conformational shifts propagate from the oligomerization domain of p53 to its tetrameric DNA binding domain and restore DNA binding to select p53 mutants, *EMBO J. 12*, 5057−5064.
22. Friedman, P. N., Chen, X., Bargonetti, J., and Prives, C. (1993) The p53 protein is an unusually shaped tetramer that binds directly to DNA, *Proc. Natl. Acad. Sci. U.S.A. 90*, 3319−3323.
23. Stenger, J. E., Tegtmeyer, P., Mayr, G. A., Reed, M., Wang, Y., Wang, P., Hough, P. V., and Mastrangelo, I. A. (1994) p53 oligomerization and DNA looping are linked with transcriptional activation, *EMBO J. 13*, 6011−6020.
24. Mirzayans, R., Bashir, S., Murray, D., and Paterson, M. C. (1999) Inverse correlation between p53 protein levels and DNA repair efficiency in human fibroblast strains treated with 4-nitroquinoline 1-oxide: Evidence that lesions other than DNA strand breaks trigger the p53 response, *Carcinogenesis 20*, 941−946.
25. Bunz, F., Dutriaux, A., Lengauer, C., Waldman, T., Zhou, S., Brown, J. P., Sedivy, J. M., Kinzler, K. W., and Vogelstein, B. (1998) Requirement for p53 and p21 to sustain G2 arrest after DNA damage, *Science 282*, 1497−1501.
26. Cho, Y., Gorina, S., Jeffrey, P. D., and Pavletich, N. P. (1994) Crystal structure of a p53 tumor suppressor−DNA complex: Understanding tumorigenic mutations, *Science 265*, 346−355.
27. Lane, D. P., and Crawford, L. V. (1979) T antigen is bound to a host protein in SV40-transformed cells, *Nature 278*, 261−263.

28. Chen, X., Ko, L. J., Jayaraman, L., and Prives, C. (1996) p53 levels, functional domains, and DNA damage determine the extent of the apoptotic response of tumor cells, *Genes Dev. 10*, 2438−2451.
29. Derossi, D., Joliot, A. H., Chassaing, G., and Prochiantz, A. (1994) The third helix of the *Antennapedia* homeodomain translocates through biological membranes, *J. Biol. Chem. 269*, 10444−10450.
30. Vives, E., Brodin, P., and Lebleu, B. (1997) A truncated HIV-1 Tat protein basic domain rapidly translocates through the plasma membrane and accumulates in the cell nucleus, *J. Biol. Chem. 272*, 16010−16017.
31. Elliott, G., and O'Hare, P. (1997) Intercellular trafficking and protein delivery by a herpesvirus structural protein, *Cell 88*, 223−233.
32. Schwarze, S. R., Ho, A., Vocero-Akbani, A., and Dowdy, S. F. (1999) In vivo protein transduction: Delivery of a biologically active protein into the mouse, *Science 285*, 1569−1572.
33. Wender, P. A., Mitchell, D. J., Pattabiraman, K., Pelkey, E. T., Steinman, L., and Rothbard, J. B. (2000) The design, synthesis, and evaluation of molecules that enable or enhance cellular uptake: Peptoid molecular transporters, *Proc. Natl. Acad. Sci. U.S.A. 97*, 13003−13008.
34. Futaki, S., Suzuki, T., Ohashi, W., Yagami, T., Tanaka, S., Ueda, K., and Sugiura, Y. (2001) Arginine-rich peptides. An abundant source of membrane-permeable peptides having potential as carriers for intracellular protein delivery, *J. Biol. Chem. 276*, 5836−5840.
35. Matsushita, M., Tomizawa, K., Moriwaki, A., Li, S. T., Terada, H., and Matsui, H. (2001) A high-efficiency protein transduction system demonstrating the role of PKA in long-lasting long-term potentiation, *J. Neurosci. 21*, 6000−6007.
36. Richard, J. P., Melikov, K., Vives, E., Ramos, C., Verbeure, B., Gait, M. J., Chernomordik, L. V., and Lebleu, B. (2003) Cell-penetrating peptides. A reevaluation of the mechanism of cellular uptake, *J. Biol. Chem. 278*, 585−590.
37. Lundberg, M., Wikstrom, S., and Johansson, M. (2003) Cell surface adherence and endocytosis of protein transduction domains, *Mol. Ther. 8*, 143−150.
38. Wadia, J. S., Stan, R. V., and Dowdy, S. F. (2004) Transducible TAT-HA fusogenic peptide enhances escape of TAT-fusion proteins after lipid raft macropinocytosis, *Nat. Med. 10*, 310−315.
39. Zelphati, O., Wang, Y., Kitada, S., Reed, J. C., Felgner, P. L., and Corbeil, J. (2001) Intracellular delivery of proteins with a new lipid-mediated delivery system, *J. Biol. Chem. 276*, 35103−35110.
40. Yuki, S., Kondo, Y., Kato, F., Kato, M., and Matsuo, N. (2004) Noncytotoxic ribonuclease, RNase T1, induces tumor cell death via hemagglutinating virus of Japan envelope vector, *Eur. J. Biochem. 271*, 3567−3572.
41. Vogelstein, B., and Kinzler, K. W. (1992) p53 function and dysfunction, *Cell 70*, 523−526.
42. Verma, I. M., and Somia, N. (1997) Gene therapy—Promises, problems and prospects, *Nature 389*, 239−242.
43. Takenobu, T., Tomizawa, K., Matsushita, M., Li, S. T., Moriwaki, A., Lu, Y. F., and Matsui, H. (2002) Development of p53 protein transduction therapy using membrane-permeable peptides and the application to oral cancer cells, *Mol. Cancer Ther. 1*, 1043−1049.
44. Zender, L., Kuhnel, F., Kock, R., Manns, M., and Kubicka, S. (2002) VP22-mediated intercellular transport of p53 in hepatoma cells *in vitro* and *in vivo*, *Cancer Gene Ther. 9*, 489−496.
45. Michiue, H., Tomizawa, K., Wei, F. Y., Matsushita, M., Lu, Y. F., Ichikawa, T., Tamiya, T., Date, I., and Matsui, H. (2005) The NH_2 terminus of influenza virus hemagglutinin-2 subunit peptides enhances the antitumor potency of polyarginine-mediated p53 protein transduction, *J. Biol. Chem. 280*, 8285−8289.
46. Maeda, T., Mahara, K., Kitazoe, M., Futami, J., Takidani, A., Kosaka, M., Tada, H., Seno, M., and Yamada, H. (2002) RNase 3 (ECP) is an extraordinarily stable protein among human pancreatic-type RNases, *J. Biochem. 132*, 737−742.
47. Hartl, F. U., and Hayer-Hartl, M. (2002) Molecular chaperones in the cytosol: From nascent chain to folded protein, *Science 295*, 1852−1858.

BI052642A

Appl Microbiol Biotechnol (2006) 73:505–511
DOI 10.1007/s00253-006-0486-3

BIOTECHNOLOGICAL PRODUCTS AND PROCESS ENGINEERING

Secretory production system of bionanocapsules using a stably transfected insect cell line

Takuya Shishido · Masaru Muraoka · Masakazu Ueda · Masaharu Seno · Katsuyuki Tanizawa · Shun'ichi Kuroda · Hideki Fukuda · Akihiko Kondo

Received: 25 March 2006 / Revised: 2 May 2006 / Accepted: 4 May 2006 / Published online: 18 July 2006

Abstract Bionanocapsules (BNCs) are hollow nanoscale particles composed of L protein of the hepatitis B virus surface antigen that represent specific affinity for human hepatocytes. BNCs can transfer genes and drugs into human hepatocytes efficiently and specifically. BNC can be expressed in yeast cells. In this study, we developed a new L particle production system using a stably transfected insect cell line. For this purpose, we established a host–vector system using the *Trichoplusia ni* insect cell line. L particles were efficiently secreted by the overexpression of the L protein, which was fused to the secretion signal peptide. The concentration of L particles was reached approximately 1.7 μg/ml in 5 days during cultivation in a serum-free medium without antibiotic selective pressure. The production of L particles was maintained for at least 75 days. The secretory production of L particles facilitated their easy purification by chromatography. Furthermore, it was demonstrated that purified L particles can transfect only human hepatocytes. Therefore, an insect cell expression system is an attractive tool for the production of BNC.

T. Shishido · A. Kondo (✉)
Faculty of Engineering, Kobe University,
Kobe 657-8501, Japan
e-mail: akondo@kobe-u.ac.jp

M. Muraoka · H. Fukuda
Graduate School of Science and Technology, Kobe University,
Kobe 657-8501, Japan

M. Ueda
School of Medicine, Keio University,
Tokyo 160-0016, Japan

M. Seno
Graduate School of Natural Science and Technology,
Okayama University,
Okayama 700-8530, Japan

K. Tanizawa · S. Kuroda
The Institute of Scientific and Industrial Research,
Osaka University,
Ibaraki 567-0047, Japan

Introduction

Viral and nonviral gene transfer vectors were developed for gene therapy (El-Aneed 2004; Helge 2000; Schmidt-Wolf and Schmidt-Wolf 2003). Viral vectors, such as adenoviruses, adenoassociated viruses, and retroviruses, have some advantages such as high transduction efficiency and stability. However, there are safety concerns for the clinical applications of viral vectors (Schroder et al. 2002; Woods et al. 2003; Li et al. 2002). On the other hand, nonviral vectors, such as naked DNA and liposomes, are generally safe and do not have a limitation in the size of the transgene. However, the efficiency of gene transfer is low (Herweijer and Wolff 2003; Hirko et al. 2003). Furthermore, these vectors transfer genes to not only the target cells but also other cells. Thus, no system has so far fulfilled the required criteria of high cell and tissue specificity, high transgene efficiency, and high safety level.

We previously reported an efficient drug and gene delivery system with L particles derived from the hepatitis B virus (HBV) (Yamada et al. 2003; Yu et al. 2005). HBV is an enveloped DNA virus of Hepadnaviridae. The human hepatocytes infected with HBV synthesize and release not only 42 nm of HBV virions but also noninfectious 22 nm empty subviral particles, which are spherical and filamentous. The HBV genome encodes three envelope proteins: the S protein, which is a major constituent (226 amino acid residues) of the HBV envelope protein and empty HBV surface antigen (HBsAg) particles; the M protein, which

contains 55 additional amino acid residues (pre-S2 peptide) at the N terminus of the S protein; and the L protein, which contains the 108 (subtype *y*) or 119 (subtype *d*) additional amino acid residues (pre-S1 peptide) at the N terminus of the M protein (Heermann et al. 1984). L particles are hollow nanoparticles consisting of only the L protein and endoplasmic reticulum membrane-derived phospholipids (Yamada et al. 2001). L particles have several advantages compared with viral and nonviral vectors. Firstly, L particles show a high infectivity. Secondly, L particles are very safe because they are free from the viral genome. Thirdly, there is no practical limitation in the size of the transgene. Because of these reasons, the applicability of L particles can be extended to the delivery of proteins and chemical compounds. Furthermore, they have specificity for human hepatocytes. The results of in vitro and in vivo transfection experiments demonstrated that genes and drugs are specifically transferred into human hepatocytes using L particles (Yamada et al. 2003). It was suggested that L particles are strongly expected as potential candidates for the specific gene and drug delivery system.

To date, the preparation of HBsAg particles was studied in various expression systems, namely, yeast cells (Valenzuela et al. 1982), mammalian cells (Holzer et al. 2003), plant cells (Richter et al. 2000), and insect cells (Lanford et al. 1989; Hofmann et al. 1995; Deml et al. 1999a,b). We previously demonstrated the efficient production of L particles in recombinant yeast cells and 4 μg of the purified L particles was obtained from 1 ml of the culture medium after 7 days of cultivation (Yamada et al. 2001; Kuroda et al. 1992). However, L particles accumulate in the cytoplasm, therefore, yeast cell disruption and a subsequent purification step are required. On the other hand, the productivity of L particles is very low in mammalian cells (>50 ng/ml). Therefore, insect cells are desired as a new expression system for the production of L particles. A transient expression system using recombinant baculoviruses was reported previously (Lanford et al. 1989; Hofmann et al. 1995). However, insect cells are killed during infection cycle in this system and expressed recombinant proteins tend to be degraded by proteases. A stable expression system in stably transfected cell lines was also reported (Deml et al. 1999a,b). Although S particles or L particles coexpressed with the S protein are produced efficiently, an expression system with only L particles has not yet been established.

In this study, we constructed a new L particle expression system. The L protein was fused to the honeybee melittin secretion signal peptide and we examined the expression of the fused protein in insect cells. The stably transfected insect cell line can efficiently produce L particles and secrete into the culture medium. This production was stable for more than 2 months. Furthermore, it was indicated that the expressed L particles can be used for gene and drug delivery.

Materials and methods

Materials and strains

The *Escherichia coli* strain NovaBlue (*endA1 hsdR17* (rk12 −/mk12+) *supE44 thi-1 recA1 gyrA96 relA1 lac* [F′ *proA+B* + *lacIqZ.M15* :: Tn*10* (TcR)]) (Novagen, Darmstadt, Germany) was used as a host for recombinant DNA manipulation. *E. coli* was cultivated in Luria–Bertani medium (1% tryptone, 0.5% yeast extract, and 1% NaCl; w/v) with 100 μg ampicillin/ml.

Cell culture

The *Trichoplusia ni* BTI-TN-5B1-4 insect cell line (High Five, Invitrogen, Carlsbad, CA, USA) was maintained in a serum-free medium (Express Five SFM, Invitrogen) supplemented with 0.26 g/l L-glutamine and 0.1% gentamicin (Invitrogen) at 27 °C. The human hepatocellular carcinoma cell line NuE was maintained in RPMI1640 medium supplemented with 10% (v/v) fetal bovine serum (FBS) at 37 °C in 5% CO_2 (Murayama et al. 1999). The human hepatocellular carcinoma cell line HepG2 and human epidermal carcinoma cell line A431 were maintained in Dulbecco's modified Eagle's medium supplemented with 10% (v/v) FBS.

Plasmids construction

The expression plasmid for the L protein was constructed by inserting a fragment of a large hepatitis B surface antigen (L protein, subtype *adr*) into pXINSECT-DEST38 (Invitrogen) and pIB/V5-His (Invitrogen). This insert was amplified from the plasmid pGLDLIIP39-RcT by polymerase chain reaction (Kuroda et al. 1992) using the forward primer 5′-GGGGGATCCACCATGAAATTCTTAGT CAACGTTGCCCTTGTTTTTATGGTCGTATA CATTTCTTACATCTATGCCATGGGGAC GAATCTTTCTGTTCCC-3′, including the honeybee melittin secretion signal peptide sequence or 5′-GGGGGATC CATGAAGTTATGCATATTACTGGC CGTCGTGGCCTTTGTTGGCCTCTCGCTC GGGATGGGGACGAATCTTTCTGTTCCCAAT-3′, including the *Drosophila* binding protein (Bip) secretion signal peptide sequence, and the reverse primer 5′-CCCGCGGCCGCGTCGACCAGCTTTAACGAACG CAG-3′. The amplified fragment was digested at the *Bam*HI and *Not*I restriction sites and ligated into plasmids pXINSECT-DEST38 and pIB/V5-His. The resulting plas-

mids were designated pX-Mel, pX-Bip, pIB-Mel, and pIB-Bip. To obtain a stable transformant, plasmid pBmA.neo (Invitrogen), which contains the neomycin resistant gene, was used simultaneously with the plasmid pX-Mel and pX-Bip.

Transfection and selection of insect cell line

For the transient expression of L particles, High Five cells were seeded on a 35-mm dish at a density of 2×10^5 cells/ml 24 h before transfection, and the cells were transfected with 1 μg of pX-Mel, pX-Bip, pIB-Mel, and pIB-Bip using FuGENE 6 (Roche, Basel, Switzerland). Three days posttransfection, culture supernatant was recovered and L particles were assayed using an IMx enzyme immunoassay (EIA) kit (Abbott Laboratories, Abbott Park, IL, USA), which can specifically detect the particulate forms of HBsAg but not the free HBsAg protein.

For the generation of stably transfected cell lines, High Five cells were cotransfected with pX-Mel and pBmA.neo or pX-Bip and pBmA.neo with weight ratios of 10:1, 50:1, and 100:1 (pX:pBmA.neo). At 48 h posttransfection, transfected cells were resuspended in 12 ml of a fresh culture medium and distributed on a 12-well plate. After 1 day, the medium was replaced with fresh Express Five SFM containing 1.0 mg/ml G418 (Invitrogen) for selection. The selective medium was replaced every 4 days, and stably transfected cell lines were isolated after 3 weeks of selection with a G418-containing medium. The concentration of L particles was assayed after 4 days of cultivation of cloned cells using an IMx EIA kit.

L particle production with stably transfected High Five cells

For the analysis of the stability of L particle expression, stably transfected High Five cells were seeded on a 12-well plate at a density of 1×10^5 cells/ml in 1 ml of a fresh medium and allowed to grow for 8 days. The concentration of L particles from the culture supernatant was assayed everyday using an IMx EIA kit. The production stability of stably transfected High Five cells was examined for 75 days. The stably transfected cells were subcultured and L particles produced were quantified at 5-day intervals.

Western blot analysis

Sodium dodecyl sulfate polyacrylamide gel electrophoresis of L particles in culture supernatants was performed using 10% gel. Western blot analysis was performed using an anti-S protein antibody prepared from an immunized mouse as the primary antibody and an alkaline phosphatase (AP)-conjugated anti-mouse IgG antibody (Promega Co., Madison, WI, USA) as the secondary antibody. The colorimetric detection of AP activity was performed using 5-bromo-4-chloro-3-indolyl-phosphate and nitro blue tetrazolium (Promega Co., Madison, WI, USA).

Purification of L particles from stably transfected cell culture supernatants

The culture supernatant (150 ml) of stably transfected insect cells was collected and concentrated fourfold by ultrafiltration using a Vivaspin20 device (Sartorius AG, Goettingen, Germany) at 4 °C. After concentration, the supernatant was loaded on sulfate Cellulofine resin (Chisso, Tokyo, Japan) equilibrated in 0.01 M sodium phosphate (pH 7.2) containing 0.15 M NaCl in a disposable gravity column (Clontech Laboratories, CA, USA), and washed. L particles were recovered by elution with 0.01 M sodium phosphate (pH 7.2) containing 0.5 M NaCl.

In vitro transfection of calcein with L particles

Calcein (0.1 mM, bis[*N,N*-bis(carboxymethyl)aminomethyl]fluorescein); Dojindo, Kumamoto, Japan) was mixed with purified L particles (240 ng) in 200 μl of phosphate-buffered saline, and electroporated into the particles using a Gene pulser II electroporation system (BioRad Laboratories, Hercules, CA, USA) in a 2-mm-gap cuvette, typically at 200 V and 1,000 μF for about 20 ms. The electroporated L particles were centrifuged at 8,000 rpm for 1.5 min and 60 ng of L particles recovered from supernatant were added to 2×10^4 cells of HepG2, NuE, and A431. Fluorescence was observed under an 5-Pa laser-scanning microscope (LSM) (Carl Zeiss, Oberkochen, Germany) at 6 h posttransfection at 37 °C.

Results

Establishment of High Five expression system of L particles

To investigate the dependence of L-particle productivity on the expression cassette, the transient expression of L particles in High Five cells was performed using pX-Mel, pX-Bip, pIB-Mel, and pIB-Bip. The expression plasmid pX contains the silkmoth (*Bombyx mori*) cytoplasmic actin gene promoter and pIB contains the promoter derived from the baculovirus *Orgyia pseudotsugata* multicapsid nuclear polyhedrosis virus (*Op*MNPV) (Fig. 1). In addition, for the efficient secretion of L particles, two types of secretion signal peptide, namely, the honeybee melittin signal peptide sequence (Mel signal) and the *Drosophila* Bip signal sequence (Bip signal), were investigated. The concentration of secreted L particles from transfected cells was deter-

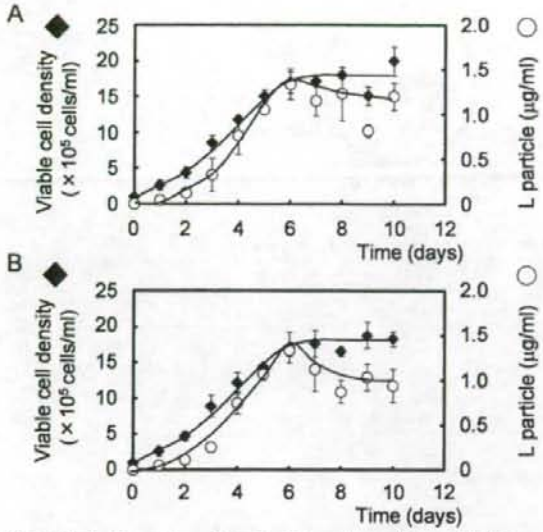

Fig. 4 Production of L particles in static culture of clone #38. Clone #38 was cultivated for 10 days with (**a**) and without G418 (**b**). The concentration of L particles in culture supernatant was determined using an IMx EIA kit. Viable cell density and L particle concentration are represented by *circles* and *diamonds*, respectively. The data points represent the average of three independent experiments

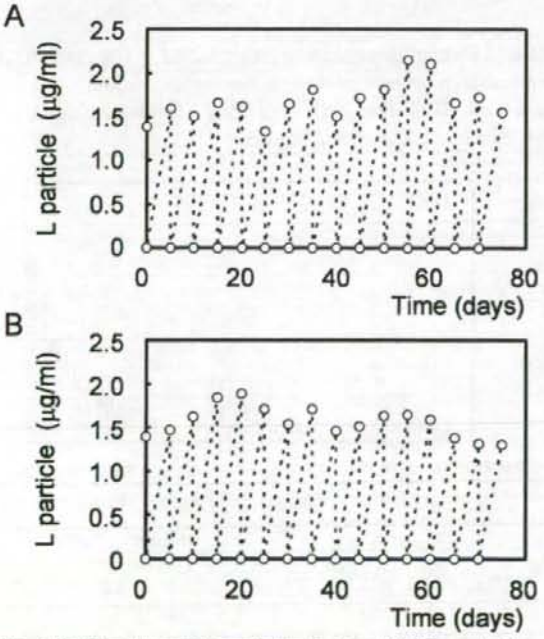

Fig. 5 Stability of L particle production in clone #38. The production stability of clone #38 was assessed every 5 days for 75 days with G418 (**a**) and without G418 (**b**)

Generation of stably transfected cell lines

High Five cells were cotransfected with pX-Mel and pBmA.neo as described in "Materials and methods." After antibiotic selection, 38 stably transfected clones were successfully obtained. Three days after the medium replacement in small static cultures, the concentration of L particles indicated the degree of heterogeneity of transformed cells (Fig. 3). The highest producer cell line (clone #38) was established by transfection at the weight ratio of 100:1 (pX:pBmA.neo). Therefore, clone #38 was used in the subsequent studies.

Production of L particle from clone #38 in static culture

Clone #38 was characterized in static batch cultures. The cells were seeded on a 12-well plate at a density of 1×10^5 cells in 1 ml of fresh medium in the presence or absence of antibiotic selective pressure (G418), and the concentration of L particles in culture supernatant was determined every day for 10 days using an IMx EIA kit. Clone #38 reached the maximum cell density of approximately 1.7×10^6 cells/ml and produced 1.3 μg/ml of L particles after 6 days of cultivation in the presence of G418 (Fig. 4a). A similar tendency was observed in the absence of G418 (Fig. 4b). These results indicated that clone #38 can produce L particles efficiently and should be subcultured to check the stability of clone #38 every 5 days at subconfluence (60–80%).

Stability of L particle production from clone #38

We confirmed the stability of clone #38, which represent high productivity of L particles in the presence or absence of antibiotic selective pressure in the long-term. The cells were subcultured every 5 days at an initial density of 1×10^5 cells/ml in a fresh medium and the culture medium was assayed for L particle production. The expression level of L particles did not change with time in the culture medium for 75 days in the presence or absence of 1.0 mg/ml G418 (Fig. 5). It is interesting to note that the average concentration of L particles reached approximately 1.7 μg/ml, which is higher than that in the static batch cultures (Fig. 4). Cell growth remained quite stable throughout the cultivation time. These results demonstrated that the stably transfected cell line showed an efficient production of L particles and the insect cell expression system was useful for vector production.

In vitro transfection of calcein with L particles

After purification by sulfate Cellulofine resin column chromatography, L particles were used for specific drug

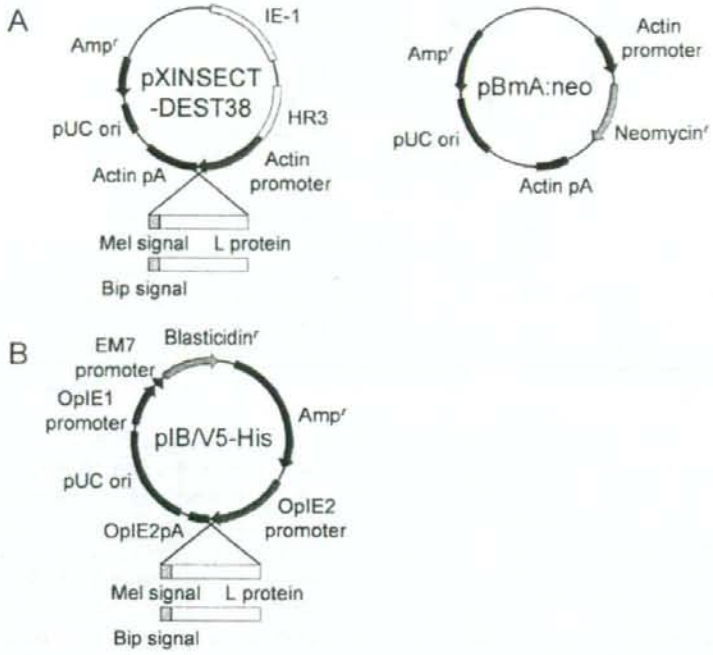

Fig. 1 Schematic representation of expression vector for L protein. One system based on pXINSECT-DEST38 including silkmoth (*Bombyx mori*) cytoplasmic actin gene promoter. In this system, pBmA.neo is used for antibiotic selection (**a**). Another system based on pIB/V5-His including promoter derived from baculovirus *Op*MNPV (**b**). The L protein was fused to the honeybee melittin secretion signal peptide and *Drosophila* Bip secretion signal peptide at its N terminus. Constructed L protein expression plasmids were named pX-Mel, pX-Bip, pIB-Mel, and pIB-Bip

mined 3 days after transfection using an IMx EIA kit (Fig. 2a). Results indicated that pX-Mel is more efficient than other expression plasmids. Furthermore, the results of Western blotting demonstrated that pX-Mel is the optimal expression plasmid for the secretory expression of L particles in High Five cells (Fig. 2b). Therefore, pX-Mel was used in the subsequent studies.

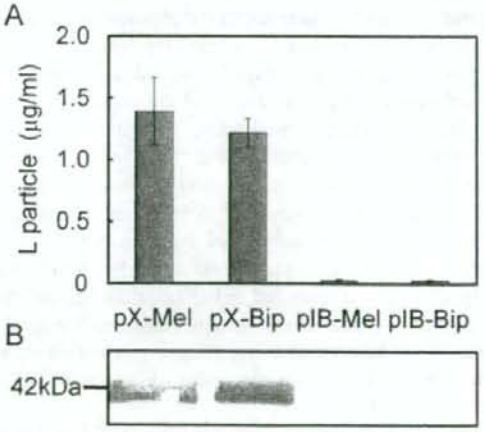

Fig. 2 Transient expression of L particles. pX-Mel, pX-Bip, pIB-Mel, and pIB-Bip were transfected into High Five cells using FuGENE 6. At 3 days after posttransfection, secreted L particles were quantified using an IMx EIA kit (**a**). The data points represent the average of three independent experiments. Western blot analysis was performed using the anti-S protein antibody (**b**)

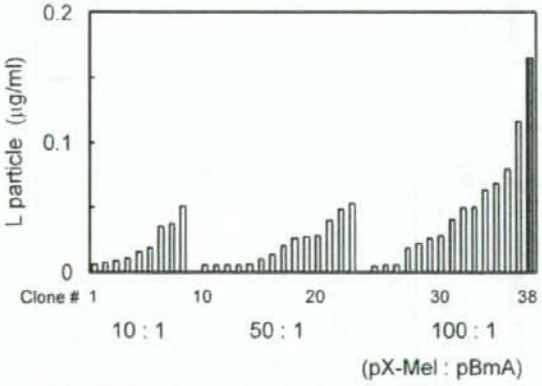

Fig. 3 Distribution of expression levels of L particles in stably transfected cell lines. High Five cells were cotransfected with pX-Mel or pX-Bip and pBmA.neo at the weight ratio of 10:1, 50:1, and 100:1 (expression plasmid pX:antibiotic resistance plasmid pBmA.neo). The amount of L particles was assayed after 3 days of subculture using an IMx EIA kit. The high-expression cell line #38 is represented by a *filled bar*

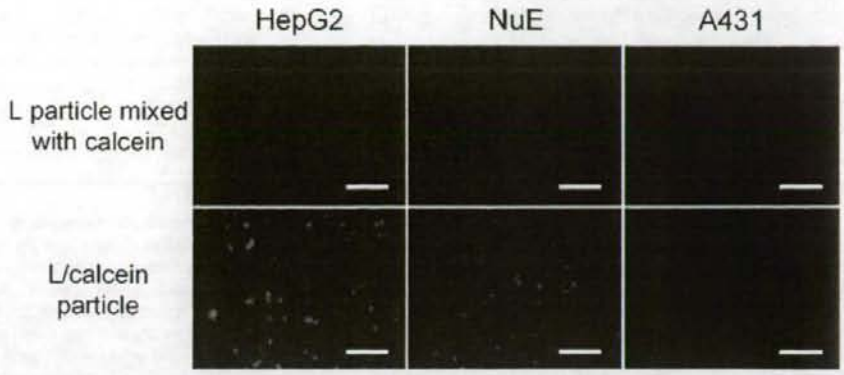

Fig. 6 Transfection of calcein with L particles. A mixture of L particles and calcein and calcein-carrying L particles (60 ng) were added to approximately 2×10^4 cells of HepG2, NuE, and A431. After 6 h of incubation at 37 °C, infection was evaluated by observing fluorescence under an LSM. *Scale bar*, 100 μm

delivery into hepatocytes. A fluorescent compound, calcein, was electroporated into L particles. The results showed that L particles can efficiently transfect the human hepatocarcinoma cell lines HepG2 and NuE (Fig. 6). On the other hand, fluorescence was not detected in the human epidermoid carcinoma cell line A431. Therefore, it was confirmed that L particles have specificity to hepatocyte and this result is consistent with the data for L particles obtained from yeast cells (Yamada et al. 2003).

Discussion

An insect cell expression system has several advantages in recombinant protein expression. The major advantage is a high level expression of secreted glycoproteins. Insect cell expression systems with HBsAg were demonstrated in previous reports. The expression of the S particle was investigated in the *Spodoptera frugiperda* Sf9 cell line using a baculovirus expression system (Lanford et al. 1989) and the stably transfected *Drosophila melanogaster* Schneider-2 (DS-2) cell line (Deml et al. 1999a,b). The coexpression of S and L proteins was achieved in the Sf9 cell line using a baculovirus expression system (Hofmann et al. 1995). However, an expression system with L particles consisting of only the L protein was not established to date except for yeast cell expression system.

We previously demonstrated that an L particle as a novel vector for the gene and drug delivery system can be prepared by overexpressing the L protein in *Saccharomyces cerevisiae* (Yamada et al. 2001; Kuroda et al. 1992). However, expressed L particles accumulate in the cytoplasm, therefore, complicated purification steps are required. Thus, we attempted to develop a stably transfected insect cell secretory expression system with L particles in this study.

To determine the host–vector system, two different systems were examined for transient expression using High Five cells, which are superior hosts for the production of recombinant proteins (Farrell et al. 1998; Keith et al. 1999). Moreover, the secretion signal peptide was fused to the L protein for the efficient production of L particles (Kuroda et al. 1992). These results indicated that the combination of pXINSECT-DEST38 and the melittin secretion signal peptide was suitable for the expression of L particles (Fig. 2). The difference in productivity between expression systems with various vectors might be attributed the nature of the promoter and the presence of homologous region 3 (HR3) and IE1 from *Bombyx mori* nuclear polyhedrosis virus in pXINSECT-DEST38 (Fig. 1a). HR3 is a viral transcriptional enhancer and it acts as a constitutive enhancer of the cytoplasmic actin promoter (Lu et al. 1997). IE1 is a viral transcriptional transactivator that stimulates L protein expression (Lu et al. 1996). Therefore, pXINSECT-DEST38 with the melittin secretion signal peptide represented high expression efficiency of L particles. The results of Western blot analysis suggested the homogeneous glycosylation of the L protein (Fig. 2b).

In this study, we successfully established the stably transfected insect cell lines for the production of L particles. The cotransfection of pX-Mel and pBmA.neo at the weight ratio of 100:1 (expression plasmid pX:antibiotic resistance plasmid pBmA.neo) produced higher L particle-expressing clones (Fig. 3). The concentration of expression vectors seemed to correlate with expression efficiency (Deml et al. 1999a). For practical applications, a long-term stability of expression of L particles is indispensable. Secretion stability was therefore continuously examined (Fig. 5). The result indicated that the expression level of L particles in clone #38 was stable for 75 days in the presence of G418 with an average concentration of approximately 1.7 μg/ml. The stable secretion of L particles for 75 days is considered to be sufficient for industrial applications. It is interesting to note that no significant difference in productivity was observed in the absence of G418. The nonrequirement of antibiotics will minimize the production cost of L particles.

The advantage of this stably transfected insect cell expression system is the secretory expression of L particles

in the serum-free medium. In the case of a mammalian cell culture system, the efficient production of L particles requires serum. On the other hand, in the case of an insect–baculovirus expression system, L particles have to be purified from cell lysates. Both systems required expensive and time-consuming purification steps to obtain pure L particles (Deml et al. 1999b). In contrast, the current system requires only chromatographic purification. Subsequently, the in vitro transfection experiment was carried out using L particles purified from an insect cell culture. It was demonstrated that L particles produced by insect cells can specifically deliver chemical compounds into human hepatocytes.

In conclusion, we established a stably transfected insect cell expression system with L particles for the first time by selecting the appropriate promoter and secretion signal peptide. L particles were efficiently secreted into the serum-free medium and facilitated an easy purification. Furthermore, it was demonstrated that L particles specifically targeted and successfully transfected human hepatocytes similarly to L particles obtained from yeast cells (Yamada et al. 2003). L particles from insect cells could be applied to specific gene and drug delivery systems, and in the preparation of HB vaccine. An insect cell expression system is an attractive tool for the production of L particles and biorecognition molecules displaying L particles for retargeting.

Acknowledgements This study was supported by grants-in-aid for Research on Advanced Medical Technology from the Ministry of Health, Labour and Welfare.

References

Deml L, Schirmbeck R, Reimann J, Wolf H, Wagner R (1999a) Purification and characterization of hepatitis B virus surface antigen particles produced in *Drosophila* Schneider-2 cells. J Virol Methods 79:205–217

Deml L, Wolf H, Wagner R (1999b) High level expression of hepatitis B virus surface antigen in stably transfected Drosophila Schneider-2 cells. J Virol Methods 79:191–203

El-Aneed A (2004) An overview of current delivery systems in cancer gene therapy. J Control Release 94:1–14

Farrell PJ, Lu M, Prevost J, Brown C, Behie L, Iatrou K (1998) High-level expression of secreted glycoproteins in transformed lepidopteran insect cells using a novel expression vector. Biotechnol Bioeng 60:656–663

Heermann KH, Goldmann U, Schwartz W, Seyffarth T, Baumgarten H, Gerlich WH (1984) Large surface proteins of hepatitis B virus containing the pre-S sequence. J Virol 52:396–402

Helge G (2000) Gene therapy—when a simple concept meets a complex reality. Funct Integr Genomics 1:142–145

Herweijer H, Wolff JA (2003) Progress and prospects: naked DNA gene transfer and therapy. Gene Ther 10:453–458

Hirko A, Tang F, Hughes JA (2003) Cationic lipid vectors for plasmid DNA delivery. Curr Med Chem 10:1185–1193

Hofmann C, Sandig V, Kirillova I, Jennings G, Rudolph M, Schlag P, Strauss M (1995) Hepatocyte-specific binding of L/S-HBV particles expressed in insect cells. Biol Chem Hoppe Seyler 376:173–178

Holzer GW, Mayrhofer J, Leitner J, Blum M, Webersinke G, Heuritsch S, Falkner FG (2003) Overexpression of hepatitis B virus surface antigens including the preS1 region in a serum-free Chinese hamster ovary cell line. Protein Expr Purif 29:58–69

Keith MB, Farrell PJ, Iatrou K, Behie LA (1999) Screening of transformed insect cell lines for recombinant protein production. Biotechnol Prog 15:1046–1052

Kuroda S, Otaka S, Miyazaki T, Nakao M, Fujisawa Y (1992) Hepatitis B virus envelope L protein particles, synthesis and assembly in *Saccharomycescerevisiae*, purification and characterization. J Biol Chem 267:1953–1961

Lanford RE, Luckow V, Kennedy RC, Dreesman GR, Notvall L, Summers MD (1989) Expression and characterization of hepatitis B virus surface antigen polypeptides in insect cells with a baculovirus expression system. J Virol 63:1549–1557

Li Z, Dullmann J, Schiedlmeier B, Schmidt M, von Kalle C, Meyer J, Forster M, Stocking C, Wahlers A, Frank O, Ostertag W, Kuhlcke K, Eckert HG, Fehse B, Baum C (2002) Murine leukemia induced by retroviral gene marking. Science 296:497

Lu M, Johnson RR, Iatrou K (1996) Trans-activation of a cell housekeeping gene promoter by the IE1 gene product of baculoviruses. Virology 218:103–113

Lu M, Farrell PJ, Johnson R, Iatrou K (1997) A baculovirus (*Bombyx mori* nuclear polyhedrosis virus) repeat element functions as a powerful constitutive enhancer in transfected insect cells. J Biol Chem 272:30724–30728

Murayama Y, Tadakuma T, Kunitomi M, Kumai K, Tsutsui K, Yasuda T, Kitajima M (1999) Cell-specific expression of the diphtheria toxin A-chain coding sequence under the control of the upstream region of the human α-fetoprotein gene. J Surg Onco 70:145–149

Richter LJ, Thanavala Y, Arntzen CJ, Mason HS (2000) Production of hepatitis B surface antigen in transgenic plants for oral immunization. Nat Biotechnol 18:1167–1171

Schmidt-Wolf GD, Schmidt-Wolf IG (2003) Non-viral and hybrid vectors in human gene therapy: an update. Trends Mol Med 9:67–72

Schroder AR, Shinn P, Chen H, Berry C, Ecker JR, Bushman F (2002) HIV-1 integration in the human genome favors active genes and local hotspots. Cell 110:521–529

Valenzuela P, Medina A, Rutter WJ, Ammerer G, Hall BD (1982) Synthesis and assembly of hepatitis B virus surface antigen particles in yeast. Nature 298:347–350

Woods NB, Muessig A, Schmidt M, Flygare J, Olsson K, Salmon P, Trono D, von Kalle C, Karlsson S (2003) Lentiviral vector transduction of NOD/SCID repopulating cells results in multiple vector integrations per transduced cell: risk of insertional mutagenesis. Blood 101:1284–1289

Yamada T, Iwabuki H, Kanno T, Tanaka H, Kawai T, Fukuda H, Kondo A, Seno M, Tanizawa K, Kuroda S (2001) Physicochemical and immunological characterization of hepatitis B virus envelope particles exclusively consisting of the entire L (pre-S1 +preS-2+S) protein. Vaccine 19:3154–3163

Yamada T, Iwasaki Y, Tada H, Iwabuki H, Chuah MK, VandenDriessche T, Fukuda H, Kondo A, Ueda M, Seno M, Tanizawa K, Kuroda S (2003) Nanoparticles for the delivery of genes and drugs to human hepatocytes. Nat Biotechnol 21:885–890

Yu D, Amano C, Fukuda T, Yamada T, Kuroda S, Tanizawa K, Kondo A, Ueda M, Yamada H, Tada H, Seno M (2005) The specific delivery of proteins to human liver cells by engineered bio-nanocapsules. FEBS J 272:3651–3660

Anti-tumor effect in an *in vivo* model by human-derived pancreatic RNase with basic fibroblast growth factor insertional fusion protein through antiangiogenic properties

Hiroshi Yagi,[1] Masakazu Ueda,[1,4] Hiromitsu Jinno,[1] Koichi Aiura,[1] Shuji Mikami,[2] Hiroko Tada,[3] Masaharu Seno,[3] Hidenori Yamada[3] and Masaki Kitajima[1]

Departments of [1]Surgery, and [2]Pathology, Keio University School of Medicine, Tokyo; [3]Department of Bioscience and Biotechnology, Faculty of Engineering, Graduate School of Natural Science and Technology, Okayama University, Okayama, Japan

(Received July 13, 2006/Revised August 23, 2006/Accepted August 27, 2006/Online publication October 18, 2006)

It is thought that the export of angiogenic fibroblast growth factors (FGF) from tumors may be involved in the onset of tumor angiogenesis. To create a new active targeting drug that inhibits the tumor angiogenic process without toxicities to normal cells, human basic FGF (h-bFGF) was inserted genetically into the Gly89 position of cross-linked RNase1 (the ribonuclease inhibitor protein [RI] binding site of cross-linked human pancreatic RNase) to prevent stereospecific binding to RI. The resultant insertional-fusion protein (CL-RFN89) was active both as h-bFGF and as RNase1. Furthermore, it acquired an additional ability of evading RI through steric blockade of RI binding caused by the fused h-bFGF domain. In the present study, the effect of the resultant protein, CL-RFN89, on the antitumor response though its antiangiogenic properties was investigated in an *in vivo* model. Continuous systemic treatment with CL-RFN89 significantly inhibited the growth of human A431 squamous cell carcinomas *in vivo*. Seven days of treatment with CL-RFN89 resulted in a 58.2% inhibition of tumor growth compared with control mice ($P < 0.0001$). Furthermore, immunohistochemistry using a rat antimouse CD31 antibody showed that treatment with CL-RFN89 reduced tumor vascularization. These findings identify CL-RFN89 as a potent systemic inhibitor of tumor growth as a result of its antiangiogenic properties. This protein appears to be a new systemic antitumor agent. (*Cancer Sci* 2006; 97: 1315–1320)

Improvement of cytotoxic agents specific to cancer cells or other cells causing proliferative diseases is one of the goals of targeted chemotherapy. Such cells often express surface receptors or other molecules distinguishing them from the surrounding normal cells. In this regard, many immunotoxins have been developed that exploit this difference. Immunotoxins are defined as proteins containing an antibody (or a ligand) and a toxin.[1,2] The antibody moiety or ligand specific for a cell surface molecule delivers the toxin to the target cells. Plant and bacterial toxins have been the most intensively studied moieties. These toxins are enzymes that catalytically abolish protein synthesis when they translocate into the cytosol. However, clinical applications are still limited owing to the inherent toxicities of these substances to normal cells, in addition to their immunogenicity. Distinct targeting specificity and humanization of immunotoxins are needed to overcome these difficulties.

There is increasing evidence that malignant tumor growth and progression are dependent on the induction of tumor angiogenesis,[3–5] and clinical studies have revealed that high vessel density often correlates with poor prognosis.[6] Angiogenesis is regulated by a fine balance between inducers and inhibitors of this process (angiogenic and angiostatic factors, respectively).[7] For tumor metastasis, it is necessary for the neoplasm to grow beyond 1–2 mm in diameter.[8] Therefore, inhibition of the angiogenic process has become one of the most promising strategies for the treatment of malignant neoplasms.

Basic fibroblast growth factor (bFGF) is a prototype member of a family of structurally related growth factors that exert important pleiotropic effects on cell differentiation and organ development *in vitro* and *in vivo*.[9–11] bFGF plays an important role in many of these processes and represents one of the most potent inducers of angiogenesis known, functioning both as an autocrine and a paracrine factor to stimulate vascular endothelial cell proliferation and migration, and induction of the expression of specific proteases, growth factors and integrins involved in angiogenesis.[12–14] As overexpression of fibroblast growth factor (FGF) receptors possibly correlates with the malignancy of tumors and bFGF is proposed to support autocrine growth of melanoma cells,[15] the receptors are potential targets for melanoma therapy.[16] In fact, chemical conjugates or fusion proteins between bFGF and saporin, a ribosome-inactivating protein isolated from the plant *Saponaria officinalis*, have been developed that show growth inhibitory effects on cells expressing FGF receptors.[17–19]

In an attempt to make fusion proteins safer for clinical use, we and others have introduced the use of mammalian enzymes such as ribonucleases (RNases) instead of bacterial toxins.[20–22] RNases constitute a large superfamily across many species.[23] Some members are cytotoxic and have antitumor activity. Mammalian RNase is non-toxic to cultured cells and can be substituted for plant or bacterial toxins as an immunotoxin.[24] Bovine pancreatic RNase A chemically conjugated to human transferrin and to antibodies to the transferrin receptor became cytotoxic specifically to those cells bearing the transferrin receptor.[20] It was shown that bovine pancreatic RNase A can selectively eliminate squamous carcinoma cells overexpressing epidermal growth factor receptors *in vitro* when chemically coupled to human epidermal growth factor (hEGF).[25] The availability of recombinant human pancreatic RNase (RNase1), the human homolog of bovine pancreatic RNase A that we cloned from human pancreas,[26] enabled us to construct a totally human chemical conjugate of hEGF and RNase1, which was found to be equally potent *in vitro*.[21] In order to stabilize RNase1 by the introduction of an intramolecular cross link, a mutant protein (4–118 CL RNase1), in which Arg4 and Val118 are replaced with cysteine residues and linked by a disulfide bond, was designed and expressed in *Escherichia coli* as inclusion bodies.[27] However, a previous study showed that in the cytosol, RNase encounters the ribonuclease inhibitor protein (RI) and is inactivated by

[4]To whom correspondence should be addressed. E-mail: m_ueda@sc.itc.keio.ac.jp

doi: 10.1111/j.1349-7006.2006.00336.x

forming a tight complex that prevents RNA substrates from entering the active sites of the enzyme.[28]

Several kinds of hybrid proteins have been constructed to produce bifunctional proteins and utilized as tools such as detectors for biological molecules. Generally, these hybrid proteins have been built by end-to-end fusion (tandem-fusion) of two genes of the component proteins. Previously, Futami *et al.* constructed cytotoxic RNase by fusing human bFGF (h-bFGF) to the C-terminus of RNase1.[29] The resultant tandem-fusion protein inhibited the growth of malignant cells expressing high levels of cell surface FGF receptor. However, its activity was still weak (IC_{50} [protein concentration that promotes a 50% inhibition of cell growth] > 1 μM), which could be due to incomplete inactivation by RI. Recently, Hoshimoto *et al.* had made des. 1–7 RNase1, which is an RNase1 variant created by mutagenesis of the DNA sequence encoding the RNase inhibitor binding site and fusion of the DNA with hEGF DNA.[30] The new protein expressed from the genetically altered DNA had reduced RNase activity but exhibited an even greater reduction in its affinity to bind RNase inhibitor. However, the protein was unstable.

The alternative is to insert the second protein (the insert protein) into the middle of the sequence of the host protein in-frame. This new mode of gene fusion (insertional-fusion) is expected to give an additional configuration between the two component domains and to make it possible to create the hybrid protein with the ideal 3-dimensional structure for new functions.[31] To create a new active targeting drug that inhibits the tumor angiogenic process without toxicities to normal cells, h-bFGF was inserted genetically into Gly89 of cross-linked RNase1 (the RI binding site of cross-linked RNase1) to prevent its stereo-specific binding to RI. The resultant insertional-fusion protein (CL-RFN89) was active both as h-bFGF and as RNase1. Furthermore, it acquired an additional ability of evading RI through steric blockade of RI-binding caused by the fused h-bFGF domain. CL-RFN89 retained more than 85% of its activity even in the presence of a 200-fold molar excess of RI and showed growth inhibitory effects on mouse B16/BL6 melanoma cells,[31] which express both bFGF and high-affinity FGF receptor.[32] Subsequently, tumor angiogenesis, which is mediated and promoted by the interaction of bFGF and the FGF receptor, was suppressed by this fusion protein.[33]

In the present study, the effect of CL-RFN89 on the antitumor response though its antiangiogenic properties was investigated in an *in vivo* model. Continuous systemic treatment with CL-RFN89 significantly inhibited the growth of human A431 squamous cell carcinomas (SCC) *in vivo*. Seven days of treatment with CL-RFN89 resulted in a 58.2% inhibition of tumor growth compared with control mice ($P < 0.0001$). Furthermore, immunohistochemistry using a rat antimouse CD31 antibody showed that the treatment with CL-RFN89 reduced tumor vascularization. These findings identify CL-RFN89 as a potent systemic inhibitor of tumor growth as a result of its antiangiogenic properties.

Materials and Methods

Cell lines. A431 SCC cells procured form Riken (Saitama, Japan) were maintained in Dulbecco's Modified Eagles Medium containing 10% fetal bovine serum. All the cells were cultured in an atmosphere of 5% CO_2 at 37°C.

Animals. Four-week-old female BALB/c (nu/nμ) mice were obtained from CLEA Japan (Tokyo, Japan). The animals were housed in an airconditioned room at 22–23°C, with free access to food and water.

Construction of CL-RFN89. Construction and purification of the insertional fusion protein CL-RFN89 has been described previously.[31] Briefly, recombinant human 4–118 cross-linked RNase1 (CL-RNase1) and human bFGF (147 amino acid form) were purified from *Escherichia coli*.[29,34] A cDNA encoding bFGF (19–146) (N-terminal 18-residue truncated form of bFGF) was amplified by polymerase chain reaction. A *Sac*II site was introduced at Gly89 of the CL-RNase1 cDNA and the cDNA was inserted into a CL-RNase1 expression vector. The resultant plasmid was cleaved with *Sac*II and ligated in-frame with the *Sac*II fragment of bFGF (19–146) to construct the expression vectors for insertional-fusion proteins.[31] All of the insertional-fusion proteins were expressed as inclusion bodies in *E. coli*, solubilized, refolded and purified as described previously.[29,31,34] The estimated molecular weight was 28.94 kDa. The purified proteins were concentrated by ultrafiltration with an Ultrafree-4 centrifugal filter (Biomax-5K NMWL; Millipore, Bedford, MA, USA). Protein concentrations were determined by ultraviolet spectroscopy as described previously.[35]

***In vivo* tumorigenesis assays.** Four-week-old, female BALB/c (nu/nμ) mice were injected intradermally with human A431 SCC cells (5×10^6) on the right flank. One day after tumor cell inoculation, mice were injected intraperitoneally with 50 μM (200 μL; 0.3 mg) of CL-RFN89, 50 μM (200 μL; 0.2 mg) of bFGF and 200 μL of phosphate-buffered saline (PBS). After injection, ALZET Osmotic Pumps (Durect, Cupertino, CA, USA) were placed subcutaneously in the left flank of each mouse (Fig. 1b). The pumps contained 200 μL (0.3 mg) of CL-RFN89 (50 μM), or 200 μL (0.2 mg) of bFGF (50 μM) alone, or 200 μL of PBS (control). The pumps released the solutions continually for 1 week (approximately 10 μM per day). There were eight mice each in the CL-RNase1 and PBS groups and four mice in the bFGF group. The smallest and largest tumor diameters were measured every day and tumor volumes were calculated using the following formula:

$$(4/3) \times \pi \times (1/2 \times \text{smallest diameter})^2 \times 1/2 \times \text{largest diameter}.$$

All tumors were resected and their weights measured.

Tumor data were analyzed by repeated measure one-way ANOVA followed by Fisher's least significant difference for multicomparison, in which each value was compared with the control value. StatView software was used for statistical calculations (Abacus Concepts, Berkeley, CA, USA).

Immunohistochemistry. For histological analysis, tumors were harvested from three additional animals per treatment group. Eleven days after the start of therapy and at the end of the observation period, they were removed, frozen rapidly and stored at −80°C. Frozen tissues were embedded in Optimal Cutting Temperature (OCT) compound and prepared by hexane quenching. After this, these frozen tumor tissues were cut into serial thin sections (4 μm) in the cryostat (−20°C). General tissue morphology was visualized and photographed with a camera (Olympus DP-50 CUl; Olympus Optical, Tokyo, Japan) mounted on a microscope (Olympus BX51 TF; Olympus Optical). Staining was carried out at room temperature throughout using the Rat ABC Staining System (SC-2019; Santa Cruz Biotechnology, Santa Cruz, CA, USA). The sections were then incubated overnight at 4°C in the presence of a rat antimouse CD31 antibody (dilution 1:100; Fitzgerald Industries International, Concord, MA, USA) (Fig. 2a1–c1). Counterstaining was carried out with Carazzi's hematoxylin (Fig. 2a2–c2) and the corresponding frozen tumor sections were also stained with hematoxylin and eosin using standard techniques (Fig. 2a3–c3).

Microvessel density was determined by computer-assisted analysis. For the analysis of tumor vessels, CD31-stained sections were imaged with a digital camera at ×100 magnification and morphometric analysis was carried out using Adobe Photoshop 7.0 (Adobe Systems, San Jose CA, USA) and Image J (Research Services Branch of the National Institute of Mental Health, Bethesda, MD, USA). At least three different fields in each section were examined for relative area occupied by tumor blood vessels, as described previously.[36] The repeated measure

doi: 10.1111/j.1349-7006.2006.00336.x

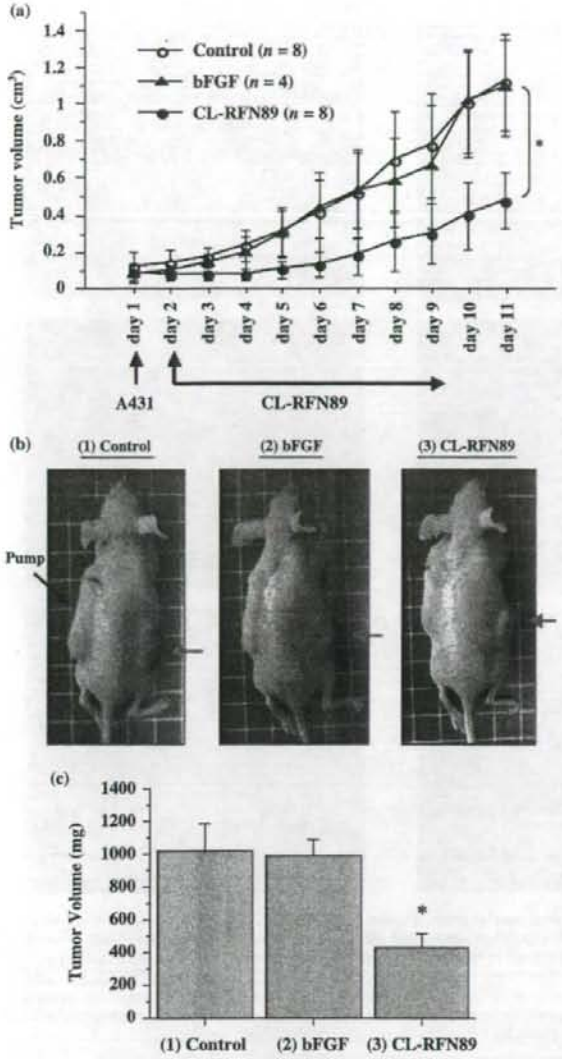

Fig. 1. Systemic therapy with CL-RFN89 inhibits tumor growth of A431 *in vivo*. One day after tumor cell inoculation, mice were injected intraperitoneally with CL-RFN89, basic fibroblast growth factor (bFGF) and phosphate-buffered saline (PBS). The pumps placed in each mouse after injection contained CL-RFN89, bFGF alone or PBS (control), and they released the liquids continually for 1 week. (a) Systemic treatment with CL-RFN89 significantly inhibited human A431 tumor growth compared with control mice (*$P = 0.0003$). Error bars show the SD. (b) The representative pictures show retarded tumor growth after CL-RFN89 treatment (3) compared with PBS-control treatment (1) and bFGF treatment (2). (c) The final mean weights of the tumors were 1018.8 ± 164.7 mg ($n = 8$) (1), 993.0 ± 96.5 mg ($n = 4$) (2) and 426.3 ± 86.3 mg ($n = 8$) (3). CL-RFN89 treatment (3) showed 58.2% inhibition of tumor growth compared with control-treated mice (1) (*$P < 0.0001$). Error bars show the SD.

one-way ANOVA followed by Fisher's least significant difference for multicomparison was used for statistical analysis; each value was compared with the control value obtained using StatView.

Results

Inhibition of *in vivo* tumor growth by systemic treatment with CL-RFN89. We first investigated whether recombinant CL-RFN89 affects tumor angiogenesis and malignant tumor growth *in vivo* with systemic delivery of CL-RFN89 by intraperitoneal injection into tumor-bearing mice. We took this approach because local intratumor or peritumor injection of antiangiogenic drugs would probably not be feasible in most human patients. A431 SCC cells were implanted intradermally into immunosuppressed mice. CL-RFN89 and bFGF treatments were initiated after 1 day and continued by osmotic pump. Mice implanted with A431 SCC cells that were injected with PBS served as a negative control. Systemic treatment with CL-RFN89 significantly inhibited *in vivo* tumor growth ($P = 0.0003$) (Fig. 1a). Seven days of treatment with CL-RFN89 resulted in a significant change; the final mean tumor weights were 1018.8 ± 164.7X mg (control) and 426.3 ± 86.3X mg (CL-RFN89), corresponding to a 58.2% inhibition of tumor growth compared with control mice ($P < 0.0001$). No inhibition of tumor growth was observed by treatment with bFGF alone at a dose that was equivalent to the dose of bFGF the mice received with CL-RFN89. The tumor volumes after treatment of bFGF alone were significantly larger compared with those from mice treated with CL-RFN89 ($P < 0.0001$); the final mean tumor weight was 993.0 ± 96.5 mg for bFGF. There was no statistically significant difference in tumor growth between mice treated with PBS and mice treated with bFGF alone (Fig. 1b,c).

All therapies were well tolerated by the animals. No differences in bodyweight or behavior were observed between the treatment groups. All animals survived until the end of the observation period unless killed. Furthermore, histology of the hematoxylin–eosin-stained sections from organs including liver, spleen, kidney, lung and heart did not reveal therapy-related toxicity.

Systemic treatment with CL-RFN89 inhibits tumor angiogenesis. We next investigated whether systemic treatment with recombinant CL-RFN89 could also inhibit bFGF-driven angiogenesis *in vivo*, as assessed by the *in vivo* tumorigenesis assays. Control and bFGF-treated mice bearing A431 SCC tumors showed tumor vasculature with remarkable heterogeneity in lumen diameters and with numerous large-caliber vessels throughout the viable parts of the tumors, assessed by analysis of CD31-positive vessels (Fig. 2a,b). In contrast, there was less tumor angiogenesis in mice treated with CL-RFN89, characterized by comparatively more homogenous small-caliber vessels (Fig. 2c). Computer-assisted image analysis of CD31-positive vessels indicated that the inhibition of angiogenesis with CL-RFN89 caused a further decrease in total vascular area to values 95% lower than those measured in control and bFGF-treated tumors ($P < 0.0001$) (Fig. 3).

Discussion

In the present study, systemic inhibition of tumor growth was evaluated in A431 SCC tumor-bearing mice using CL-RFN89, a novel insertional fusion protein consisting of h-bFGF inserted into the Gly89 position of cross-linked RNase1, which was expected to inhibit RNase inhibitor interreaction. Futami *et al.* showed that cell lines expressing FGF receptors were inhibited in their growth by micromolar concentrations of RNase1–h-bFGF fusion proteins.[29] In contrast, no growth inhibition was observed in A431 cells that did not express FGF receptors.

Tumor-bearing mice received intraperitoneal injections of 50 μM of CL-RFN89 (50-fold concentration of that used in the *in vitro* assay) and subcutaneous continuous injection using an osmotic pump for 7 days with 10 μM (10-fold concentration of that used in the *in vitro* assay) of CL-RFN89 each day. It was found that CL-RFN89 significantly inhibited the growth of

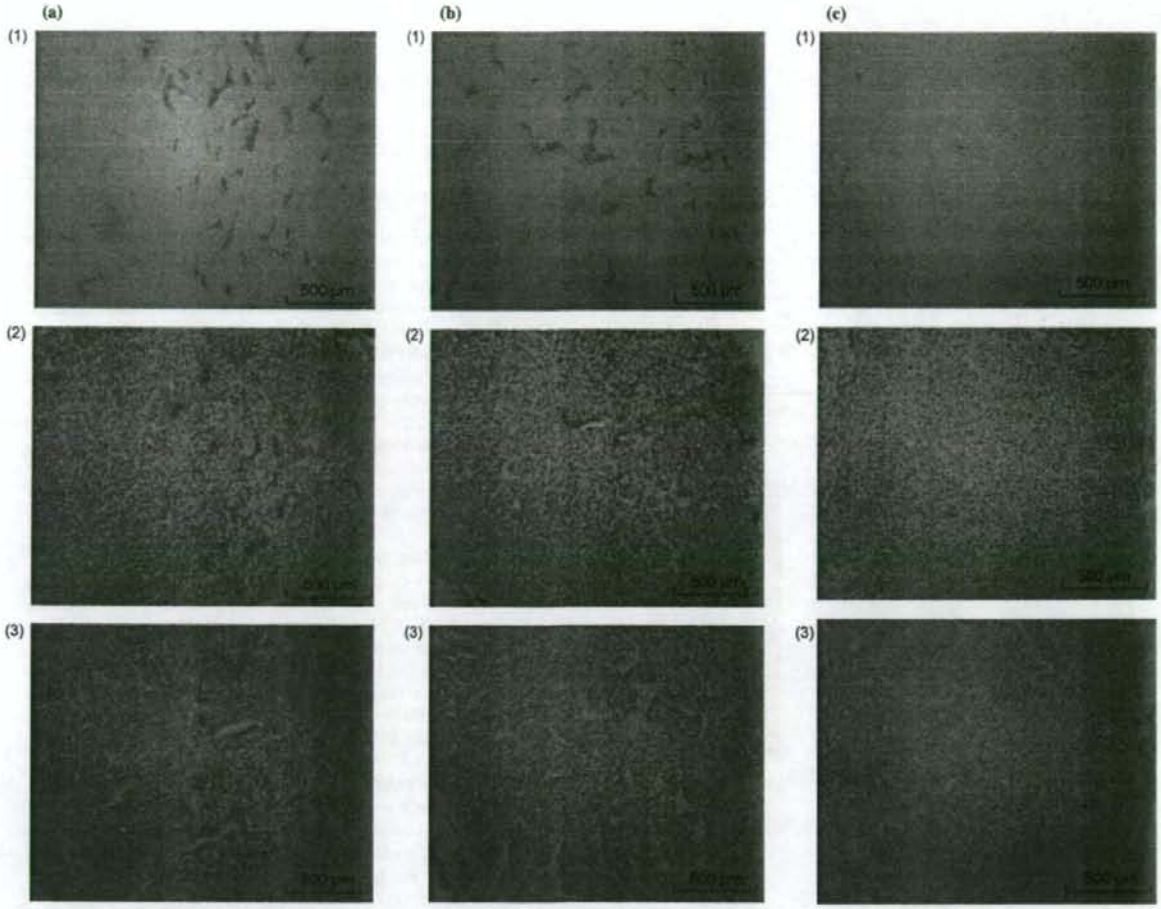

Fig. 2. Immunohistochemistry of A431 tumors. Tumor cell proliferation and microvessel density were assessed by CD31 immunostaining of A431 tumors excised on day 11 after the start of therapy. Mice were treated with phosphate-buffered saline (PBS) (control), basic fibroblast growth factor (bFGF) alone or CL-RFN89 as shown in Fig. 1. (1) The sections were incubated in the presence of a CD31 antibody. (2) Counterstaining was carried out using Carazzi's hematoxylin. (3) Corresponding frozen tumor sections were also stained with hematoxylin and eosin. (a) Control and (b) bFGF-treated A431 squamous cell carcinoma showed remarkable heterogeneity in lumen diameter with numerous large-caliber vessels throughout the viable parts of the tumors, as assessed by analysis of CD31-positive vessels. (c) In contrast, the extent of tumor angiogenesis in tumors of mice treated with CL-RFN89 was less pronounced and was characterized by more homogenous small-caliber vessels.

A431 (58%). In contrast, tumors that were treated with an equivalent dose of h-bFGF as CL-RFN89 showed no significant difference in volume compared with the tumors from mice treated with PBS (control). Also, our results suggested that h-bFGF itself had no direct antitumor activity for A431 tumors *in vivo*. However, computer-assisted analysis of tumor vessels stained with a rat antimouse CD31 antibody revealed a significant reduction of tumor vascularization after treatment with CL-RFN89.

With regard to these results, there are a number of questions to be clarified as to how this new insertional-fusion protein, CL-RFN89, acts as an antitumor agent. CL-RFN89 binds to FGF receptors on the surface of cells through the specificity of h-bFGF. It is then internalized into the cytosol where RNaseI exterts its cytotoxic effects. The mechanism of ribonuclease-mediated cytotoxicity is not known in detail.[37–39] To demonstrate internalization of RNase1 into the cytosol, Futami *et al.* used fluorescence-labeled RNase1 derivatives.[40] Tada *et al.* then showed IC_{50} values of wild-type RNase1, tandem-fusion RNase1–h-bFGF and CL-RFN89 in terms of their growth inhibitory effect on mouse melanoma B16/BL6 cells,[31] which express high-affinity FGF receptor.[32] Wild-type RNase1 activity was almost completely cancelled in the presence of RI and its IC_{50} value could not be detected. In contrast, both of the fusion proteins inhibited the growth of B16/BL6 melanoma cells, and the IC_{50} value of CL-RFN89 was five-fold lower then that of tandem-fusion RNase1–h-bFGF. These results suggested that the cytotoxicity of CL-RFN89 was caused not by internalization of RNase1 itself but by internalization of CL-RFN89 with an evasion of RI binding through steric blockade after an interaction on the plasma membrane of a target cell.

In addition, Hayashida *et al.* demonstrated that CL-RFN89 worked specifically by intervention of bFGF–FGF receptor interaction on A431 tumor.[33] Using fluorescence-labeled protein they showed that CL-RFN89 could adhere to the surface of human umbilical vein endothelial cells (HUVEC). However, in the presence of an excess amount of unlabeled h-bFGF, no adhesion or uptake of CL-RFN89 occurred. This means that the excess bFGF occupies the FGF receptors and competitively

doi: 10.1111/j.1349-7006.2006.00336.x

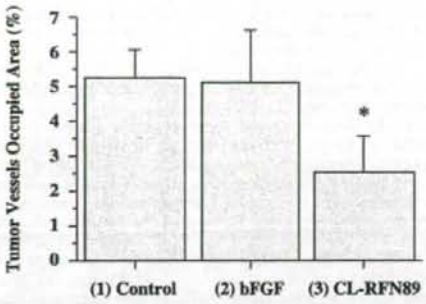

Fig. 3. Computer-assisted image analysis of CD31-positive vessels indicated that the inhibition of angiogenesis with CL-RFN89 ($n = 11$) caused a further decrease in total vascular area to values 95% lower (*$P < 0.0001$) than those measured in control ($n = 11$) and basic fibroblast growth factor (bFGF)-treated tumors ($n = 12$). Error bars show the SD.

prevents CL-RFN89 from binding to the cells, which suggests that the binding of the protein to HUVEC is FGF receptor dependent. Also, they showed that CL-RFN89 inhibited the growth of HUVEC in a dose-dependent manner. These previous results showed that CL-RFN89 was active both as h-bFGF and as RNase1.

There is one question remaining, and that is whether the inhibition of A431 tumor growth is based solely on the antiangiogenic property of the molecule. Tumor growth and metastasis are dependent on angiogenesis.[41] A tumor must continuously stimulate the growth of new capillary blood vessels for it to grow. Furthermore, the new blood vessels embedded in a tumor provide a gateway for tumor cells to enter the circulation and to metastasize to distant sites, such as liver, lung or bone. There are several angiogenic polypeptides such as bFGF, acidic fibroblast growth factor, vascular endothelial growth factor, transforming growth factor and angiogenin, with several reports describing how neovascularization of tumors is part of the genetically based tumor progression and bFGF is strongly correlated with this mode of vascularization.[7,8,42] Hori *et al.* demonstrated that solid tumor growth could be suppressed by inactivation of bFGF alone *in vivo*.[43] They prepared anti-bFGF neutralizing monoclonal antibodies as a bFGF inhibitor and showed that it could suppress tumor angiogenesis. This result suggests that bFGF is one of the most important factors in tumor angiogenesis. In addition, Hayashida *et al.* showed that CL-RFN89 had no direct cytotoxicity against A431 cells *in vitro*, but had an antiangiogeneic response *in vitro* and *in vivo* using HUVEC and in the mouse dorsal air sac assay, which suggested that CL-RFN89 is functioned as an anti-bFGF agent.[33] In the present study, the computer-assisted analysis showed a significant reduction in tumor vascularization *in vivo* after treatment with CL-RFN89. Both the previous results and our results did not completely deny the possibility of indirect action with respect to antiangiogenic activity on progenitor cells, but supported the view that the most important influence was the inhibitory effect of CL-RFN89 in tumor growth by suppression of angiogenesis, and that the effect is exerted through FGF–FGF receptor interactions on cells bearing FGF receptors, such as endothelial cells, with a role in neovascularization.[33]

Though it would be helpful if the *in vivo* distribution of CL-RFN89 was shown, we did not try to visualize it in the present study. This was because we thought that the biological half-life of CL-RFN89 might be less then 24 h, and that when CL-RFN89 accumulated in the cells bearing FGF receptors (such as endothelial cells) they would become apoptotic. It therefore seemed difficult to visualize the accumulation of this protein.

Compared with other immunotoxins, this new insertional-fusion protein, CL-RFN89, is expected to be less toxic to humans because the components are human-derived and appear to have a higher stability and RI-evading ability. In support of these statements, this new protein has several important characteristics as follows: (1) it is made from both human RNase and human bFGF; and (2) it is based on a 3-dimensional structural design that allows insertion of bFGF into cross-linked RNase1 at the exact RI-binding site. In addition, the dose of this protein needed for systemic treatment was approximately 50-fold that used in the *in vitro* assay, and was considered an acceptable dose to use *in vivo*. Also, this macromolecular agent would have an advantage compared with other micromolecular drugs. Noguchi *et al.* reported that there was a great difference in the clearance rate between solid tumors and normal tissues in the early phase of accumulation of macromolecules in tumors.[44] They showed that higher molecular weight copolymers had significantly higher tumor accumulation, whereas the lower molecular weight copolymers were cleared rapidly from tumor tissue due to rapid diffusion back into the bloodstream. Also, Dreher *et al.* investigated how molecular weight influenced the accumulation of a model macromolecular drug carrier in tumors using dextran.[45] They concluded that increasing the molecular weight of dextran significantly reduced its tumor vascular permeability, and dextrans of 40 and 70 kDa had the highest accumulation in solid tumors but were largely concentrated near the vascular surface. These results suggest that macromolecular drugs such as CL-RFN89 have higher accumulation in targeted tumors and lower toxicity to normal cells than micromolecular drugs such as the tyrosine kinase inhibitors.

These findings identify CL-RFN89 as a potent systemic inhibitor of tumor growth as a result of its antiangiogenic properties. This protein appears to be a new systemic antitumor agent.

Acknowledgments

The authors thank Mrs Yuki Nakamura and Mr Toshihide Muramatsu from the laboratory of Keio University School of Medicine and Mr Yasushi Saze, Mrs Mariko Koshiba and Ms Kazuko Nakayama from Hino Municipal Hospital for their technical support and helpful discussions. This research was supported by a Ministry of Education, Culture, Sports, Science and Technology Grant-in-Aid for Scientific Research (B) and a Grant-in-Aid for the 21st Century Center of Excellence (COE) Program entitled 'Establishment of individualized cancer therapy based on comprehensive development of minimally invasive and innovative therapeutic methods (Keio University)'.

References

1 Lappi DA, Baird A. Mitotoxins: growth factor-targeted cytotoxic molecules. *Prog Growth Factor Res* 1990; **2**: 223–36.
2 Pastan II, Kreitman RJ. Immunotoxins for targeted cancer therapy. *Adv Drug Deliv Rev* 1998; **31**: 53–88.
3 Folkman J. New perspectives in clinical oncology from angiogenesis research. *Eur J Cancer* 1996; **32**: 2534–9.
4 Hanahan D, Folkman J. Patterns and emerging mechanisms of the angiogenic switch during tumorigenesis. *Cell* 1996; **86**: 353–64.
5 Hanahan D, Christofori G, Naik P, Arbeit J. Transgenic mouse models of tumour angiogenesis: the angiogenic switch, its molecular controls, and prospects for preclinical therapeutic models. *Eur J Cancer* 1996; **32**: 2386–93.
6 Weidner N, Folkman J. Tumoral vascularity as a prognostic factor in cancer. *Important Adv Oncol* 1996: 67–190.
7 Risau W. Mechanisms of angiogenesis. *Nature* 1997; **386**: 671–4.
8 Folkman J, Shing Y. Angiogenesis. *J Biol Chem* 1992; **267**: 10931–4.
9 Klagsbrun M. The fibroblast growth factor family: Structural and biological properties. *Prog Growth Factor Res* 1989; **1**: 207–35.
10 Mason I. The ins and outs of fibroblast growth factors. *Cell* 1994; **78**: 547–52.
11 Bikfalvi A, Klein S, Pintucci G, Rifkin D. Biological roles of fibroblast growth factor-2. *Endocr Rev* 1997; **18**: 26–45.